1. Introduction

A fundamental property of baroclinic wave disturbances is the tendency for synoptic scale variations in the thermal and wind fields to become concentrated into narrow transition zones known as frontal zones. Such zones are characterized by large horizontal temperature gradients in the across front direction, a region of enhanced static stability, local maxima in vertical vorticity, and strong vertical wind shear. These frontal zones characteristically have widths on the order of 100 km, with lengths on the scale of 1000 km. Though baroclinic zones with these frontal characteristics can exist throughout the entire depth of the troposphere and lower stratosphere, they are particularly robust near the Earth's surface (referred to as surface fronts) where an impermeable solid boundary exists and at upper-levels (referred to as upper-level fronts) near the *thermodynamic* boundary represented by the tropopause.

Upper-level frontal zones are of substantial scientific and operational interest as they are associated with a variety of natural phenomena, several of which are not traditionally thought of as “weather.” For instance, the intensity and location of upper-level fronts are of considerable relevance to aircraft operations. These features are not only of concern for passenger safety related to the avoidance of regions of Clear Air Turbulence (CAT), but also for economical flight routing in terms of fuel consumption (Keyser and Shapiro, 1986). Upper-fronts are also important for understanding atmospheric chemistry, as they represent regions of small scale turbulent mixing and consequently play a significant role in the mass exchange between the troposphere and stratosphere in the mid-latitudes (Andrews et al.

1987). Within an upper-front, an intrusion of stratospheric air can mix chemical trace species, as well as radioactive debris, deep into the troposphere (Andrews et al., 1987).

Numerous studies have suggested that upper-level troughs, jets and fronts are intimately linked with the development of the extra-tropical cyclones and severe convection that bring much of the weather (in the traditional sense of the word) to the mid-latitudes (e.g. Reiter, 1969; Danielsen, 1974; Uccellini and Johnson, 1979; Uccellini et al., 1985). Specifically, extra-tropical cyclogenesis is usually the result of the circulation associated with such upper-level features. In fact, work by Sanders (1988) and Lackmann et al. (1997) (to be detailed later) makes the case that such important upper-level precursor disturbances are very often direct consequences of the upper frontogenesis process itself.

a. A historical review of upper-fronts.

The conceptual model of the structure of an upper-level front has gone through considerable evolution since the Norwegian Cyclone Model first introduced the notion of deep knife-like frontal boundaries, with zero-order temperature discontinuities, extending from the surface to the tropopause (Bjerknes and Solberg, 1922). By the 1920s, the introduction of upper air soundings made it possible to directly observe the free atmosphere. Bjerknes (1926) suggested that there was no evidence for the assumed zero-order temperature discontinuity aloft, rather the discontinuity was of first-order, in the temperature gradient and not the temperature field itself. This finding introduced the concept of a frontal zone, which replaced the theory of a frontal surface. Radiosonde analysis by Bjerknes and Palmen (1937)

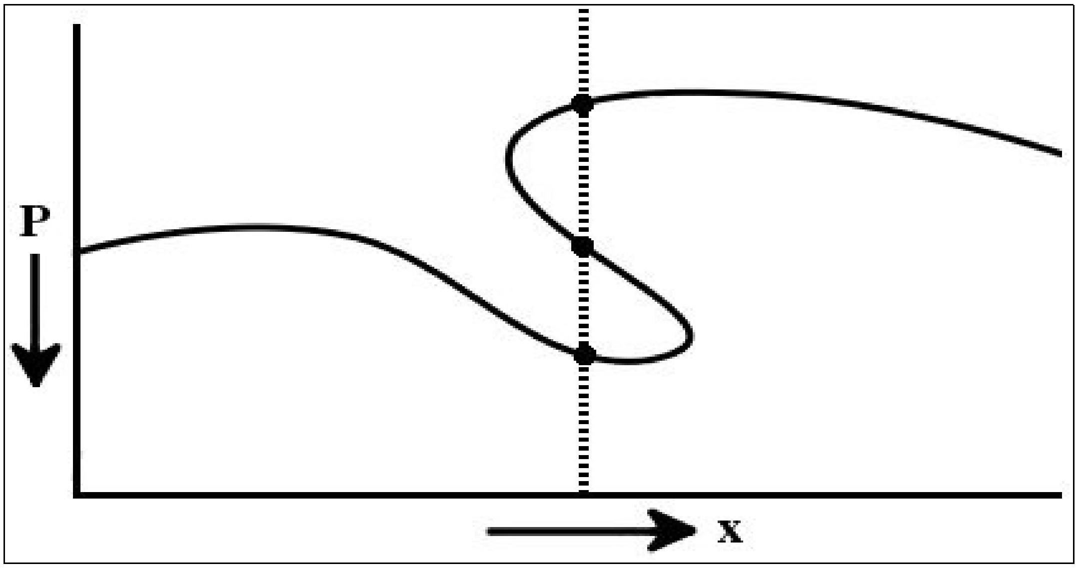

Figure 1.1: A schematic illustration of a vertical cross section through a tropopause fold, in which the tropopause (solid line) height is multi-valued over some location allowing stratospheric air to reside beneath tropospheric air.

depicted such upper-level baroclinic zones as the vertical extension of the polar front that separated polar air from tropical air throughout the depth of the troposphere. At the upper extent of this frontal zone, the horizontal temperature gradient became diffuse and the tropopause folded vertically into a characteristic S-shape illustrated schematically in Fig. 1.1.

Palmen (1948) described the mid-latitude belt of westerly jets as the most ubiquitous feature of the instantaneous flow at 500 hPa. When compared to the mean wind field, however, these jet features seemed to disappear, suggesting they were transitory features of the upper-level flow. Palmen was further intrigued by the strong temperature concentration that migrated with this belt of westerlies and the pronounced correlation between the horizontal gradient in temperature and the wind velocities at 500 hPa. He suggested that changes in the velocity field and temperature fields in frontal development take place simultaneously and were the result of the same process. Furthermore, he proposed that this process was the result of a cross-stream vertical circulation superimposed on the zonal motion.

Palmen and Nagler (1949) sought to give a detailed synoptic description of the three-dimensional structure of such strong disturbances in the upper-level westerlies. They noted that the temperature difference between the equator and the North Pole was roughly 35-40°C at 500 hPa, with approximately 50% of the difference concentrated within 1000 km in the mid-latitudes, consistent with a prior analysis by Hess (1948). This conclusion suggested to them that it was correct to regard these bands of large temperature contrast on upper air charts as real frontal zones. They noted that these upper-fronts seemed to disappear at the level of maximum wind, roughly the 300 hPa level. They further noted the existence, at 200 hPa, of a second temperature gradient, with a direction opposite and magnitude similar to its 500 hPa counterpart. From their analysis of these temperature fields, they suggested that the gradients were largely influenced by temperature changes not associated with horizontal advection. Using an isentropic analysis to recover the vertical displacements along an approximate trajectory of the flow, they concluded that the flow descended from ridge to trough and ascended from trough to ridge. They were cautious in making any further conclusions about the vertical displacements along the flow, stating that complete three-dimensional air motion in disturbances of this type must be left for further investigations. However, they did suggest that superimposed upon this general pattern of descent and ascent along the flow was a cross-stream vertical circulation. It was a combination of these types of vertical motions, they suggested, that could naturally have a strong influence on the weather and on the evolution of such upper-level baroclinic zones.

This analysis of the vertical motion field in the vicinity of upper-fronts was the first of its kind. Although not directly stated, Palmen and Nagler (1949) alluded to the idea that the vertical motion could be separated into along- and across-front components (later referred to as shearwise and transverse components, respectively). Such an idea, in reference to the generation and evolution of upper-level fronts, would not be revisited for nearly fifty years. The research constituting this thesis will explore this suggestion in considerable detail.

b. Cross-front theory

The notion, suggested by Palmen (1948) and Palmen and Nagler (1949), that cross-front vertical motions might lie at the heart of the upper-front problem caught the attention of scientists in the early 1950s. The pioneering work of Reed and Sanders (1953) and Reed (1955) pursued this idea and suggested that upper-level fronts and their associated folded tropopause structures were ubiquitous features of the mid-latitude atmosphere. Reed and Sanders (1953) noted that differential subsidence was indeed responsible for intensifying the horizontal temperature gradient associated with such features and described it as being distributed in couplets straddling the front itself. Thus, they claimed that the basic mechanism in the creation of an upper-level front was isentropic tilting due to this cross-front distribution of vertical motion. In an extension to this work, Reed (1955) examined the evolution of potential vorticity on isentropic surfaces throughout the development of a characteristic upper-front and concluded that the upper frontal boundary included a considerable amount of air of stratospheric origin. He noted that differential subsidence across the front was part of an indirect circulation that could pull a thin wedge of stratospheric air deep into the troposphere, thus explaining the so-called tropopause fold (Fig. 1.1). Reed (1955) concluded that these upper-fronts separated stratospheric air from tropospheric air, not polar from tropical air as had originally been thought. He also claimed, but did not systematically demonstrate, that the intensification of upper-fronts was frequently linked with the development of cyclones.

During frontogenesis the thermal wind relationship requires that increases in the magnitude of the potential temperature gradient must be associated with an acceleration of the geostrophic vertical shear vector. Such accelerations of the shear vector are accompanied by transverse couplets of net column divergence or convergence forced by transverse ageostrophic motion, as implied by Sutcliffe (1939). Thus, positive horizontal frontogenesis must be accompanied by a thermally direct ageostrophic vertical circulation operating transverse to the geostrophic vertical shear. A two-dimensional version of the geostrophic momentum approximation, introduced by Eliassen (1948), was first used by Sawyer (1956) and Eliassen (1962) to derive a streamfunction equation for this ageostrophic transverse circulation. This equation, known as the *Sawyer-Eliassen equation*, was the first to make the direct connection between horizontal frontogenetic forcing and the production of the transverse circulation. Their work proposed that frontogenesis was a two step process. First, the primary geostrophic (shearing and stretching) deformation acts to tighten the temperature gradient, forcing the secondary ageostrophic vertical circulation. Second, the transverse secondary ageostrophic circulation advects temperature and momentum across the frontal zone, which further intensifies the temperature gradient and horizontal shear of the frontal zone.

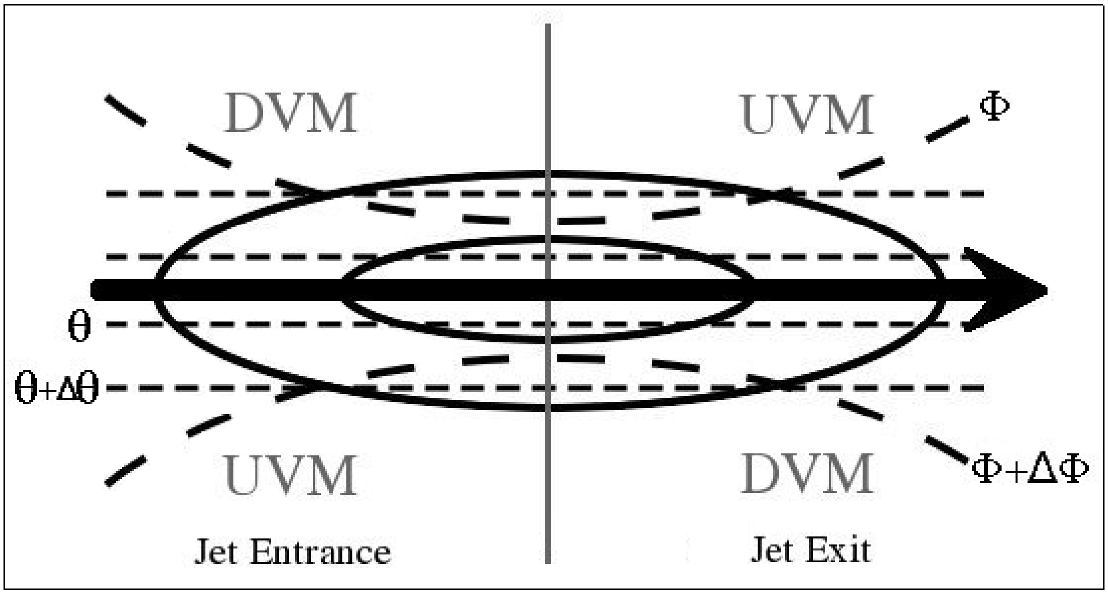

Figure 1.2: A schematic illustration of the four-quadrant model of an idealized upper-level jet streak on an isobaric surface. The left and right sides of the entrance and exit regions of the jet streak create the four quadrants. The geostrophic confluence (diffluence) in the entrance (exit) region of the jet streak, forces a thermally direct (indirect) circulation that assigns each quadrant a characteristic type of vertical motion. The jet streak, defined by the isotachs (solid lines), is oriented along the isentropes (short-dashed lines) and in the direction of the black arrow. Geostrophic confluence (difluence) is implied by the geopotential height lines (long-dashed lines). Upward (downward) vertical motion is labeled as UVM (DVM).

Bjerknes (1951) suggested that the geostrophic deformation present in the entrance and exit regions of a straight jet streak resulted in direct and indirect transverse circulations, respectively. His work resulted in the well known representation of an upper-level jet-front system, *the four-quadrant model*, illustrated in Fig. 1.2. Several studies (including Reed and Sanders 1953, Reed 1955, Bosart 1970, Shapiro 1970) noted the isentropic tilting effect as the dominant forcing for upper-level frontogenesis, which suggested that the direct circulation found in the jet entrance region would contribute to a weakening of the upper baroclinic zone. These studies further suggested that an intensifying upper-front would exhibit a transverse circulation in an indirect sense, with maximum subsidence on the warm side of the frontal zone, such as that found in the jet exit region. Shapiro (1981) noted several studies (e.g.

Hoskins and Bretherton 1972) describing intensifying upper-fronts that demonstrated increases in upper-level baroclinicity in regions of thermally direct circulations. In these cases, horizontal confluent deformation dominated the frontogenesis process. Shapiro suggested that the subsiding branch of the direct circulation could strengthen and shift toward the warm side of an intensifying upper-front when cold air advection occurred along the jet, in the presence of cyclonic shear. As a result, the circulation along the baroclinic zone could appear to be locally indirect, with subsidence maximized on the warm side of the upper-front. Thus, geostrophic temperature advection along the jet can alter the classic four-quadrant distribution of vertical motion associated with an upper-level jet-front. Shapiro (1982; his Fig. 6) schematically illustrated several combinations of stretching and shearing deformation patterns that determine the position of total geostrophic forcing and secondary vertical circulations relative to the upper-level jet-front system (Fig. 1.3).

Understanding of the evolution of an upper-level jet-front system is complicated further when these systems propagate through slower moving baroclinic waves. Shapiro (1982; his Fig. 7) presented the first conceptual model of an idealized propagating jet-front system (Fig. 1.4) by compiling results of numerous past studies, which he noted only described instantaneous segments of this interactive process. He described the formation of the jet-front in the confluence region of the polar and mid-latitude flow (Fig. 1.4a), then its progression to the inflection point in northwesterly flow, where the jet-front system is characterized by pervasive cold air advection (Fig. 4.1b). Roughly two days after its formation, Shapiro suggests that the jet-front reaches the trough axis of a fully developed baroclinic wave (Fig. 1.4c). By 72-hours, the jet front becomes situated in the southwesterly

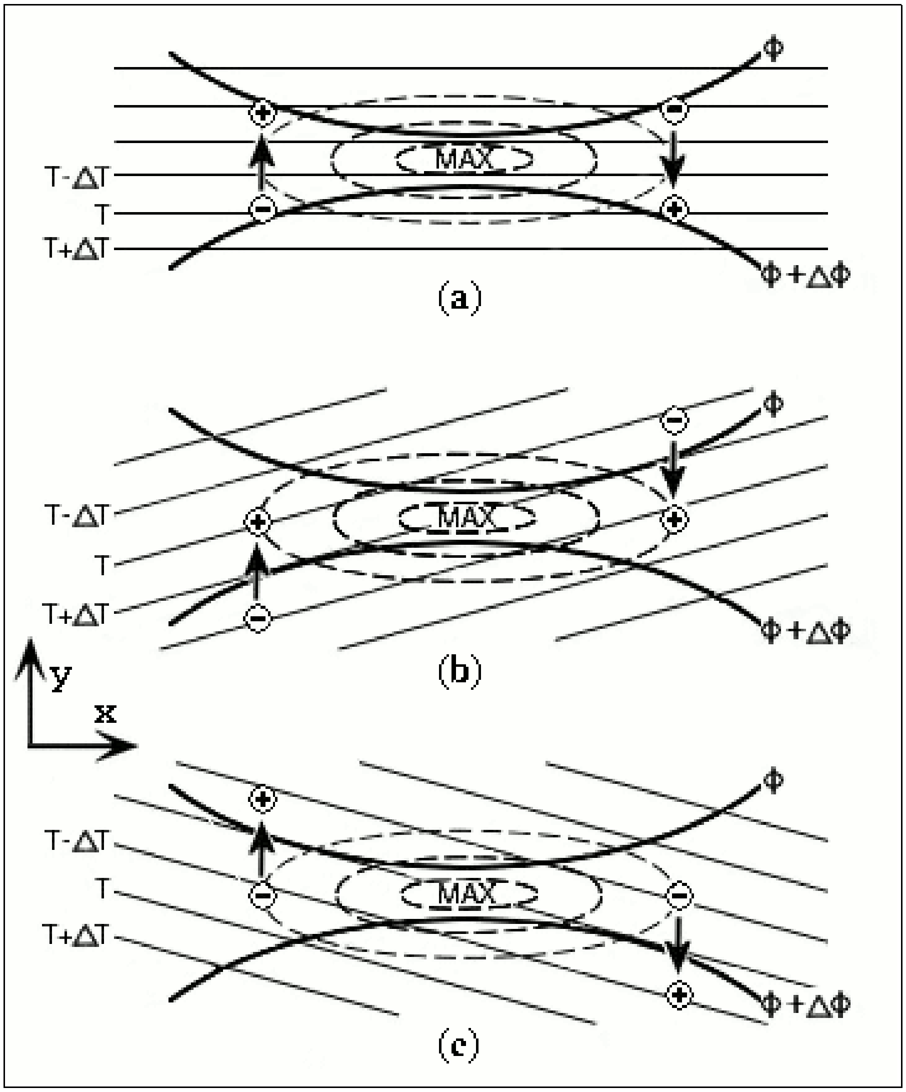

Figure 1.3: A schematic illustration, on an isobaric surface, of the changes to the idealized straight jet streak conceptual model in the presence of cold and warm air advection implied by the geopotential height (heavy solid lines), temperature (thin solid lines), isotachs (dashed lines), direction of the cross-front agostrophic wind (arrows), and sign of pressure-coordinate vertical motion (ω, plus and minus signs). (a) Straight jet streak in the absence of thermal advection, pure stretching deformation. (b) Stretching and shearing deformation with along jet cold air advection, (c) same as (b), but with warm air advection. Adapted from Shapiro (1982).

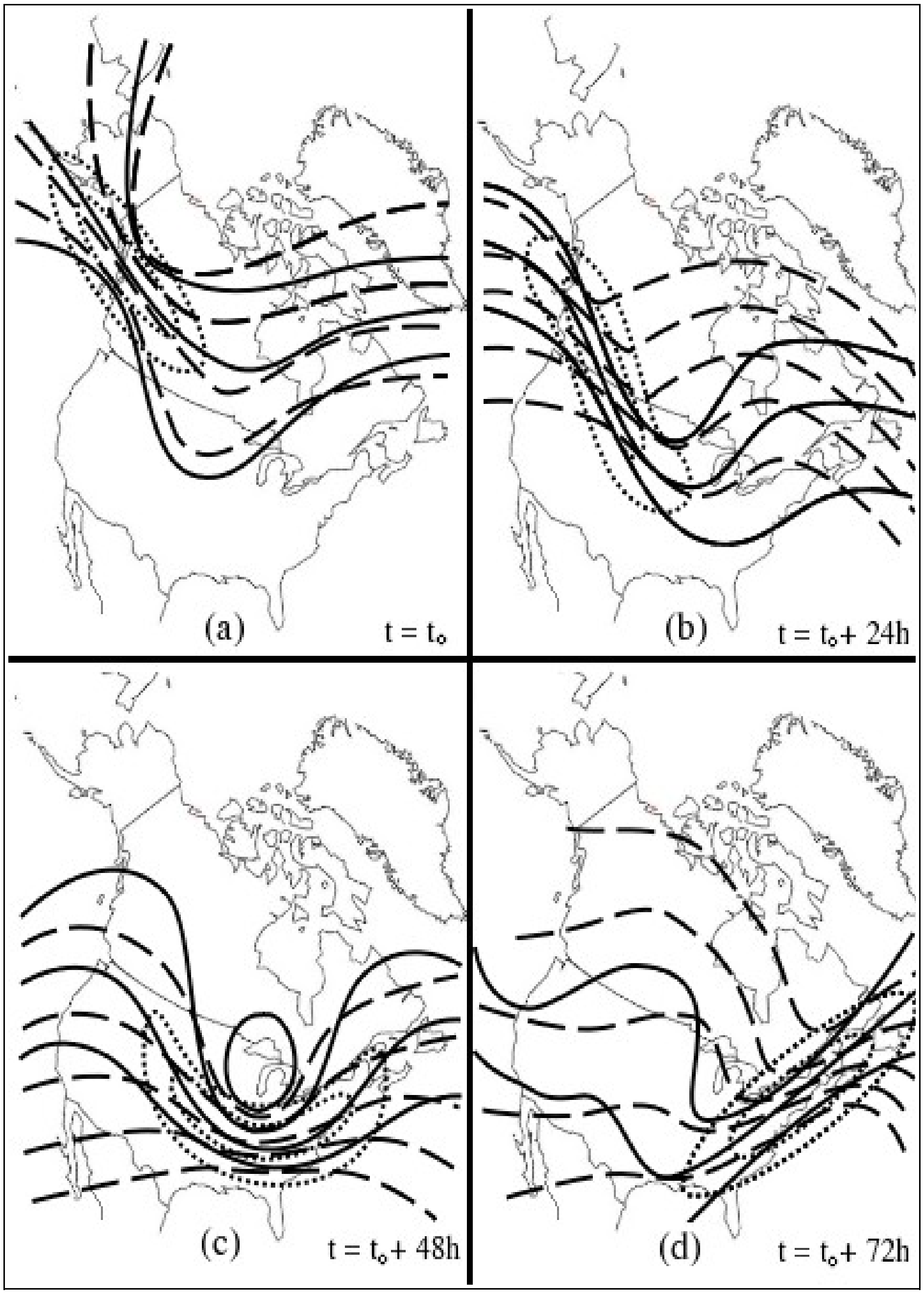

Figure 1.4: An idealized depiction of upper-level jet-front system, on a isobaric surface, propagating through a mid-latitude baroclinic wave over a 72 hour period represented by geopotential height contours (solid lines), isotachs (dotted lines), and potential temperature (dashed lines). (a) Formation of jet-front at $t=t_o$. (b) The jet-front in northwesterly flow at $t=t_o+24$-hours. (c) The jet-front reaches the trough axis at $t=t_o+48$-hours. (d) The jet-front situated in the southwesterly flow at $t=t_o+72$-hours. Adapted from Shapiro (1982).

flow inflection point of the new decaying wave, in a region of warm air advection (Fig. 1.4d). He suggested that the secondary circulations, forced by the three-dimensional variations of geostrophic motions and the thermal field, were a function of the position of the jet-front system within the baroclinic wave. The differential forcing within the wave resulted from modifications to the straight jet streak conceptual model introduced by flow curvature and thermal advection patterns.

c. Along-front theory

Numerous studies examine whether straight jet streak dynamics and the geostrophic momentum approximation are applicable to cases in which a jet-front system is embedded in a baroclinic wave. Beebe and Bates (1955) were the first to study the effects of centripetal acceleration, resulting from flow curvature, with respect to the straight jet streak conceptual model. In a later study, Newton and Persson (1962) found that the ageostrophic velocities resulting from centripetal acceleration in a sharply curved trough or ridge were of the same order as the velocity of the jet in which they were embedded. Shapiro and Kennedy (1981; their Fig. 1) provided a schematic of the idealized divergence patterns associated with pure transverse ageostrophic motion (of a straight jet) and pure along-stream ageostrophic motion (of a curved jet) (Fig. 1.5). These patterns of divergence were directly associated with the two types of vertical circulations first suggested by Palmen and Nagler (1949).

Recently, there have been multiple studies of the three-dimensional modifications, induced by flow curvature, to the two-dimensional transverse circulation captured by the Sawyer-Eliassen equation. The work of Newton and Trevisan (1984a) used a beta-plane

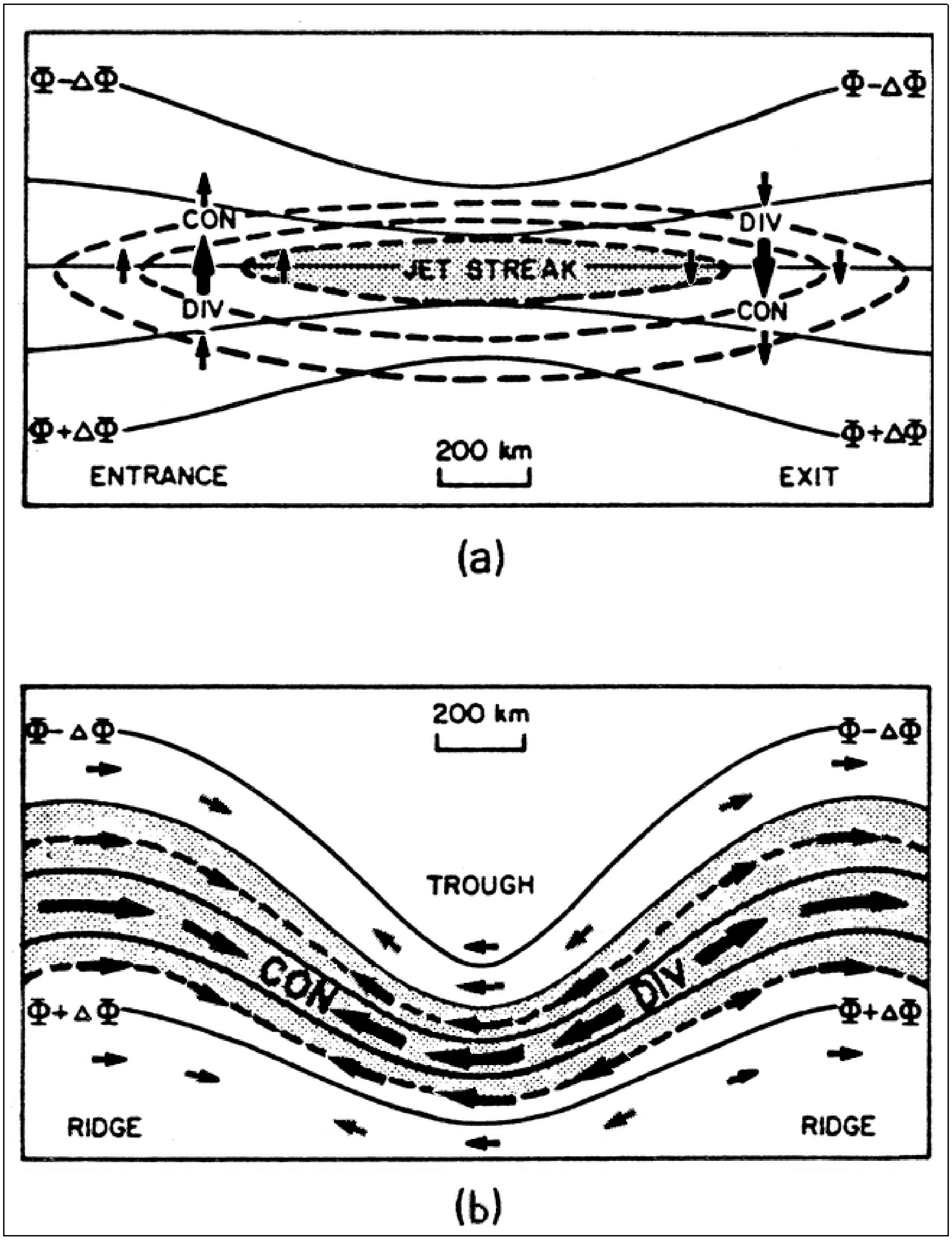

Figure 1.5: (a) A schematic representation of a straight jet streak in the absence of temperature advection producing purely transverse ageostrophic motions (arrows) and associated divergent (DIV) and convergent (CON) patterns. Solid lines are schematic geopotential heights and dashed lines are corresponding isotachs with the shaded region representing the jet maximum. (b) A uniform jet stream within a stationary synoptic wave producing purely streamwise ageostrophic motions (arrows) and associated divergent (DIV) and convergent (CON) patterns. Solid lines are schematic geopotential heights and dashed lines are corresponding streamlines with the shaded region representing the jet maximum. Adapted from Shapiro and Kennedy (1981).

primitive equation model to show the frontogenetical influence of along-front ageostrophic motion in the absence of an ageostrophic transverse circulation. They suggested that a combination of transverse and curvature-induced circulations accounted more completely for frontogenesis than did either type of circulation alone. In the second part of their work, Newton and Travisan (1984b) examined a jet-front system positioned at the base of a trough and demonstrated that the midtropospheric vertical motion pattern appeared to be a combination of transverse and curvature-induced circulations. They noted that subsidence was maximized on the warm side of the front, upstream of a trough axis, while ascent was maximized on the cold side of the front, downstream of trough axis. The numerical simulation described by Cammas and Raymond (1989), suggested that, in cases of sharply curved troughs, curvature effects of the along-stream flow in the entrance region of a jet-front system could predominate to such a point that the direct transverse circulation would not appear in the vertical velocity field.

Previous examinations of the transverse and along-stream components of the total vertical motion field during the development of upper-fronts have been purely qualitative. A significant breakthrough in quantifying these two types of vertical motion came with the work of Keyser et al. (1992a,b). Keyser et al. (1992a) provided a QG generalization of the Sawyer-Eliassen equation applicable to three-dimensional flow. Their ageostrophic streamfunction equation included the forcing for a vertical circulation found in two orthogonal planes corresponding to the cross-front and along-front directions of an idealized baroclinic disturbance. In a subsequent study, Keyser et al. (1992b) demonstrated that partitioning the $\vec{Q}$ -vector into along and across isentrope components successfully described the forcing for two orthogonal components of the total quasi-geostrophic (QG) vertical motion (ω) field. One component produced elongated (often banded) couplets of vertical motion oriented parallel to the geostrophic vertical shear, the traditional transverse couplets which will be denoted as ω_n. The other component produced cellular dipoles of vertical motion aligned along the geostrophic vertical shear. Such couplets, were referenced as shearwise couplets by Martin (2006) and will be denoted as ω_s.

Keyser et al. (1992b) proposed that an extension of their work should involve partitioning the vertical motion in observed baroclinic flow regimes. In recent work, Martin (2006, 2007) provided exactly such an extension by examining the evolution of the partitioned vertical motion field in the life cycles of two extratropical cyclones. Such a partitioning, however, has not yet been applied to analysis of the evolution of the vertical motion field associated with a developing upper front/jet system.

d. Thesis objectives

It is clear from this brief history that vertical motion plays a key role in the development of upper-fronts. Early work suggested that the dominant forcing for upper-level frontogenesis came from the differential vertical motions associated with the transverse frontal circulation. However, more recent research has documented the significant contribution to the vertical motion field made by flow variations along the front (i.e. along the geostrophic vertical shear vector). This thesis will apply the partitioned QG omega perspective, described by Keyser et al. (1992b), to quantitatively investigate the development of a robust upper-front over North America, specifically examining the distribution and role that each component of the QG vertical motion has on the evolution of an upper-front as it progresses through a baroclinic wave.

To begin the discussion, Chapter 2 provides a detailed background on the quantification of upper frontogenesis and the method of partitioning QG omega. A discussion of the important work on northwesterly flow upper frontogenesis by Schultz and Doswell (1999) completes the historical review of upper-fronts. The case analysis begins with the synoptic overview of a particularly robust upper-front traveling through an amplifying baroclinic wave, from 11 to 13 November 2003, and is described in Chapter 3. The QG vertical motion, and its components, associated with the evolution of this robust upper-front are described in Chapter 4. Chapter 5 provides the analysis and discussion of the QG vertical motion fields during the life-cycle of this upper-front. Finally, Chapter 6 summarizes the findings of this research.

2. Frontogenesis and Vertical Motion

In an attempt to quantify the intensification of a frontal zone, Petterssen (1936) developed the traditional frontogenesis equation,

$$F = \frac{d}{dt}\left|\nabla_H \theta\right|, \tag{2.1}$$

which considered the rate of change of the magnitude of the horizontal potential temperature gradient produced through advection by the horizontal wind only ($\mathbf{V}_H = u\mathbf{i} + v\mathbf{j}$). This was consistent with the then-current notion that frontogenesis could be usefully evaluated only at the surface of the Earth, where vertical motion was considered negligible. Miller (1948) noted that the increased number of upper air observations, which had extended the conceptual model of fronts into three-dimensions, required a similar broadening of the concept of frontogenesis. Thus, the Miller (1948) frontogenesis equation was the three-dimensional extension of (2.1), in which the advecting wind also included the vertical motion ($\mathbf{V} = \mathbf{V}_H + \omega\mathbf{k}$). In spite of this extension, understanding of the process of frontogenesis remained incomplete. The Miller formulation remained only a measure of the instantaneous rate of change of the *magnitude* of the potential temperature gradient. The potential temperature gradient, however, is a vector with a magnitude and direction, both of which should be considered in a frontogenesis equation.

Keyser et al. (1988) provided just such a generalization of the Petterssen frontogenesis equation, by examining the Lagrangian rate of change of the *magnitude* and *direction* of the horizontal potential temperature gradient vector,

$$\boldsymbol{F} = \frac{d}{dt}\nabla\theta. \tag{2.2}$$

In their formulation, they considered the effect of the horizontal wind only, so that

$\frac{d}{dt} = \frac{\partial}{\partial t} + u\frac{\partial}{\partial x} + v\frac{\partial}{\partial y}$. Keyser et al. (1988) exploited this conceptual extension of $\boldsymbol{F}$ by considering components using a natural coordinate system, defined by the local orientation of the isentropes in the horizontal plane such that $\hat{\boldsymbol{n}}$ was directed across the isentropes toward colder air and $\hat{\boldsymbol{s}}$ was 90° clockwise of $\hat{\boldsymbol{n}}$. In such a coordinate frame, $\boldsymbol{F} = F_s\,\hat{\boldsymbol{s}} + F_n\,\hat{\boldsymbol{n}}$. Frontogenetic forcing in the $\hat{\boldsymbol{n}}$ direction was referred to as *scalar* frontogenesis or F_n. This type of forcing was associated with a modification of the *magnitude* of the potential temperature gradient and was equivalent to Miller's frontogenesis equation. Frontogenetic forcing in the $\hat{\boldsymbol{s}}$ direction was referred to as *rotational* frontogenesis or F_s. This type of forcing resulted in the rotation and modification of the *direction* of the potential temperature gradient vector. These two components provided a complete diagnosis of the rate of change of the *magnitude* and *direction* of the potential temperature gradient.

Following the work of Keyser et al. (1988), Keyser et al. (1992b) applied the quasi-geostrophic (QG) assumption to $\boldsymbol{F}$. They noted that the so-called $\vec{\boldsymbol{Q}}$ vector, introduced by Hoskins et al. (1978), was the QG form of (2.2). For horizontal adiabatic flow,

$$\boldsymbol{Q} = \frac{d}{dt_g}\nabla_p\theta, \tag{2.3}$$

where $\frac{d}{dt_g} = \frac{\partial}{\partial t} + u_g\frac{\partial}{\partial x} + v_g\frac{\partial}{\partial y}$ and p represents differentiation on a constant pressure surface. They extended the natural coordinate partitioning onto $\vec{\boldsymbol{Q}}$, where $\vec{\boldsymbol{Q}} = Q_s\,\hat{\boldsymbol{s}} + Q_n\,\hat{\boldsymbol{n}}$

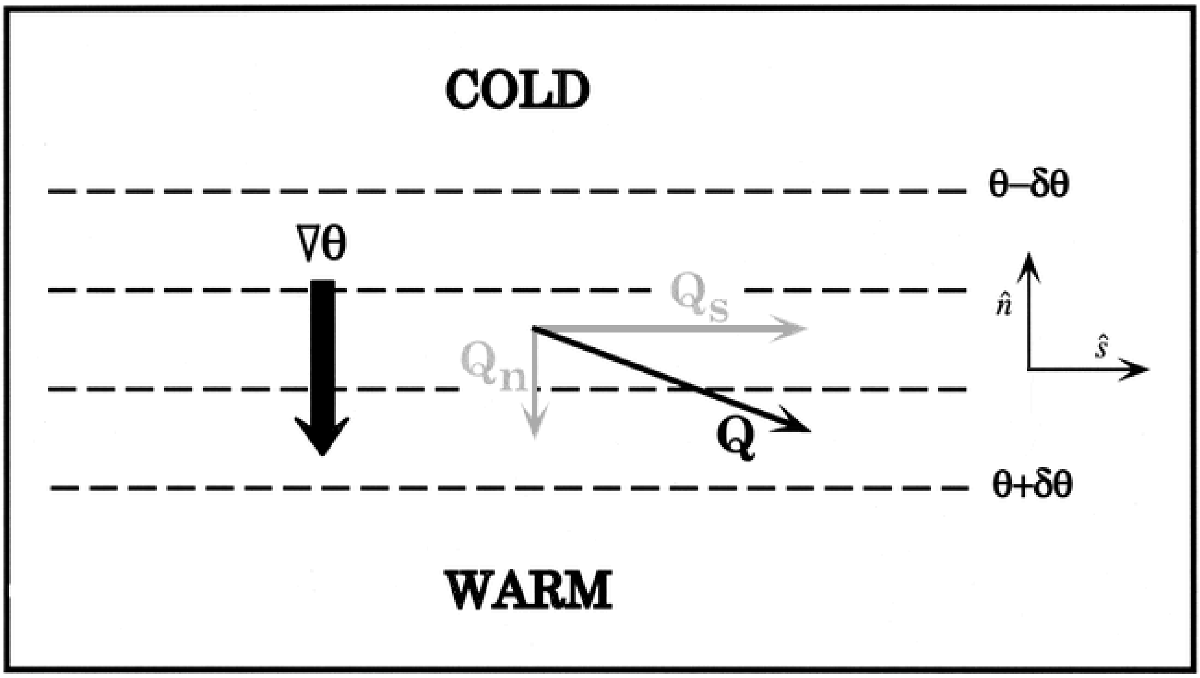

*Figure 2.1: A schematic of the natural coordinate partitioning of the **Q**-vector (thin black arrow). The dashed lines represent isentropes on an isobaric surface. $\boldsymbol{Q_n}$ is oriented across the isentropes in the same direction as the $\nabla\theta$ (bold arrow) and $\boldsymbol{Q_s}$ is oriented along the isentropes.*

(Fig. 2.1). The across isentrope component of $\vec{\boldsymbol{Q}}$ ($\vec{\boldsymbol{Q}}_n = Q_n\,\hat{\boldsymbol{n}}$) describes the rate of change of the *magnitude* of the $\nabla\theta$ following the geostrophic wind and has a magnitude given by,

$$Q_n = \left(\frac{Q\cdot\nabla\theta}{|\nabla\theta|}\right), \text{ with } \hat{\boldsymbol{n}} = -\frac{\nabla\theta}{|\nabla\theta|}. \tag{2.4}$$

The along isentrope component of $\vec{\boldsymbol{Q}}$ ($\vec{\boldsymbol{Q}}_s = Q_s\,\hat{\boldsymbol{s}}$) describes the rate of change of the *direction* of the $\nabla\theta$ following the geostrophic wind and has a magnitude given by

$$Q_s = \frac{Q\cdot(k\times\nabla\theta)}{|\nabla\theta|}, \text{ with } \hat{\boldsymbol{s}} = \frac{k\times\nabla\theta}{|\nabla\theta|}. \tag{2.5}$$

One of the original motivations for the partitioning of $\boldsymbol{F}$ was to refine the examination of the relationship between rotational and scalar frontogenesis and their associated vertical motions. Keyser et al. (1992b) exploit the QG omega equation (Hoskins et al. 1978),

$$\left(\sigma\nabla^2+f_o^2\frac{\partial^2}{\partial p^2}\right)\omega=-2\,\nabla\cdot\boldsymbol{Q}, \tag{2.6}$$

which captures the vertical motion (ω) forced by the divergence of the QG equivalent of $\boldsymbol{F}$, the $\vec{\boldsymbol{Q}}$ vector. The static stability is given by $\sigma = -(RT_o/\mathrm{P}\theta_o)(\partial\theta_o/\partial p)$, where T_o and θ_o are the domain-averaged temperature and potential temperature at each isobaric level, respectively. Using the partitioned $\vec{\boldsymbol{Q}}$ vector, the separate QG omega fields associated with rotational and scalar QG vector frontogenesis can be isolated. With the aid of a highly idealized, two-dimensional, primitive equation model, they showed that the divergence of both components of $\vec{\boldsymbol{Q}}$ were directly associated with characteristic signatures in the vertical motion fields. For several idealized representations of a baroclinic vortex, the QG forcing associated with $\vec{\boldsymbol{Q}}_s$ produced cellular dipole patterns of vertical motion on the scale of the baroclinic disturbance, which they termed wave-scale. The forcing associated with $\vec{\boldsymbol{Q}}_n$ produced banded dipole patterns of vertical motion straddling, and on the scale of, the regions of enhanced baroclinicity, which they referred to as frontal-scale. Figure 2.2 illustrates positive $\vec{\boldsymbol{Q}}_s$ and $\vec{\boldsymbol{Q}}_n$ and the associated wave-scale and frontal-scale QG vertical motion couplets, which they referred to as ω_s and ω_n, respectively. They concluded that the use of the QG vector frontogenesis function, as embodied in the $\vec{\boldsymbol{Q}}$ vector form of the QG omega equation, would appear to be the more complete alternative for inferring vertical motions associated with frontogenesis processes.

Keyser et al. (1992b) and Martin (2006) have exploited the natural coordinate partitioning of the $\vec{\boldsymbol{Q}}$ vector to examine the distribution and physical roles played by the two

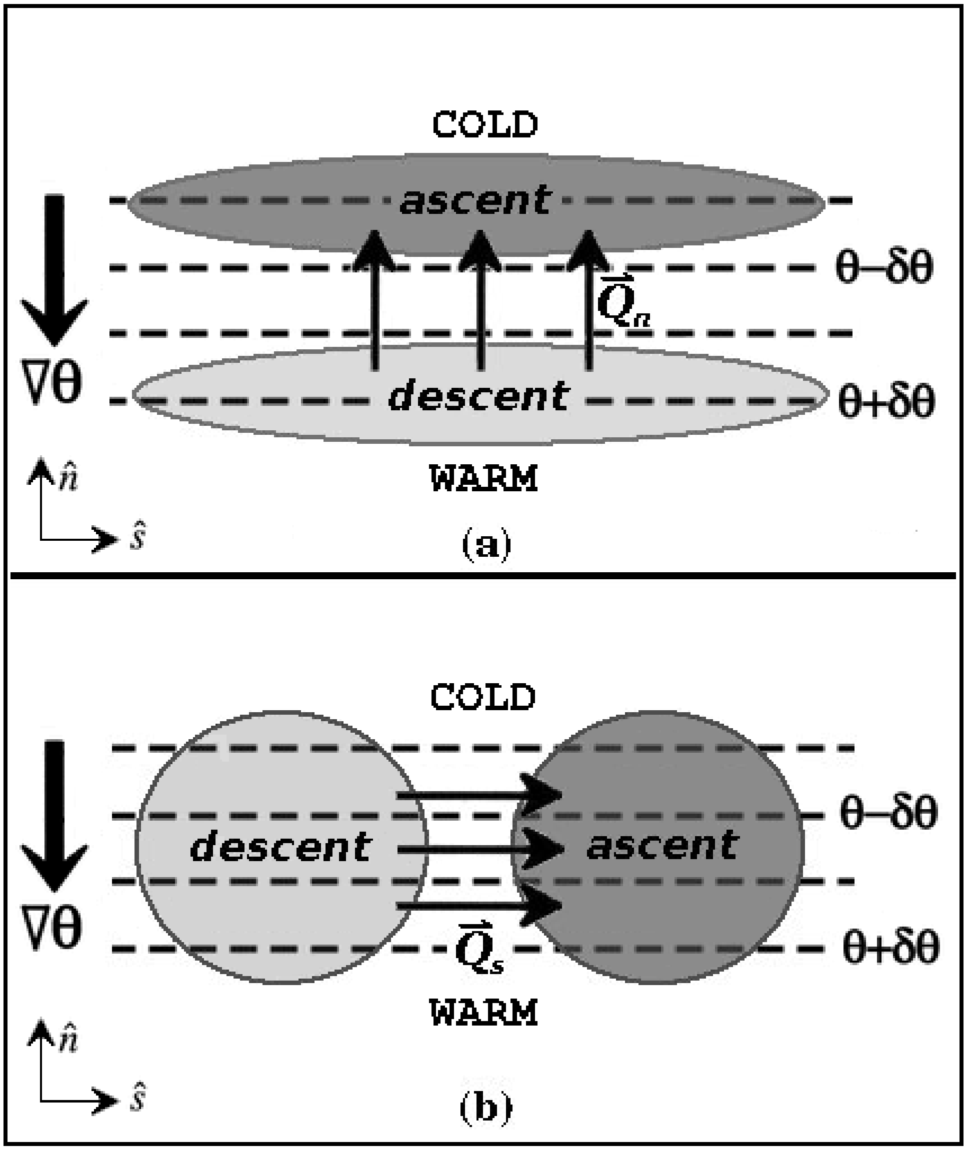

*Figure 2.2: A schematic on an isobaric surface of ω_n and ω_s couplets corresponding to $\boldsymbol{Q_n}$ and $\boldsymbol{Q_s}$ vectors, respectively. Thick dashed lines represent isentropes, dark (light) shading represents ascent (descent), and thin arrows represents the direction of the **Q**-vector components. (a) A couplet of ω_n straddling the baroclinic zone, associated with the divergence of $\boldsymbol{Q_n}$. This couplet of ω_n is associated with negative scalar frontogenesis and a decrease in the magnitude of the potential temperature gradient. (b) A couplet of ω_s oriented along the baroclinic zone, associated with the divergence of $\boldsymbol{Q_s}$. This vertical motion couplet represents the secondary circulation associated with a cyclonic rotation of the isentropes in a region of positive rotational frontogenesis.*

components of partitioned QG omega in the mid-latitude cyclone life-cycle. Keyser et al. (1992b) suggested that the characteristic comma shape of the cloud distribution in a mature mid-latitude cyclone resulted from distortion of the wave-scale dipole pattern of ω_s, by frontal-scale asymmetries of ω_n. Martin (2006, 2007) examined the contributions of both QG omega components throughout the life-cycle of a typical mid-latitude cyclone. He found that the lower tropospheric cyclogenesis was associated with the column stretching and subsequent vorticity production in the updraft portion of the ω_s couplet. Conversely, he found that the contribution of ω_n played little role in the initial development of the surface cyclone. Thus, it was suggested that cyclogenesis slightly precedes surface frontogenesis, and ω_s vertical motion dominates the initial lower tropospheric cyclone development.

Schultz and Doswell (1999) provided insight into upper-level frontogenesis and the initiation of regions of cold air advection along upper baroclinic zones. Cold air advection in regions of cyclonic shear is known to produce frontogenetic vertical tilting, a process referred to as the *Shapiro Effect* and also a characteristic of upper-level frontogenesis. Employing the natural coordinate version of $\vec{\boldsymbol{Q}}$ described by Sanders and Hoskins (1986),

$$\vec{\boldsymbol{Q}} = \frac{R}{p}\left|\frac{\partial T}{\partial n}\right|[\hat{k}\times\frac{\partial \vec{V}_g}{\partial s}], \tag{2.7}$$

cold air advection in such a shear zone mandates that the $\vec{\boldsymbol{Q}}$ must cross the isentropes from warm to cold, as depicted in Fig. 2.3. Schultz and Doswell (1999) extended the work of Keyser et al. (1988) by introducing the important effects of horizontal gradients of vertical velocity to (2.2). Using their three-dimensional extension to the vector generalization of the Petterssen frontogenesis function, they expanded both rotational and scalar frontogenesis into

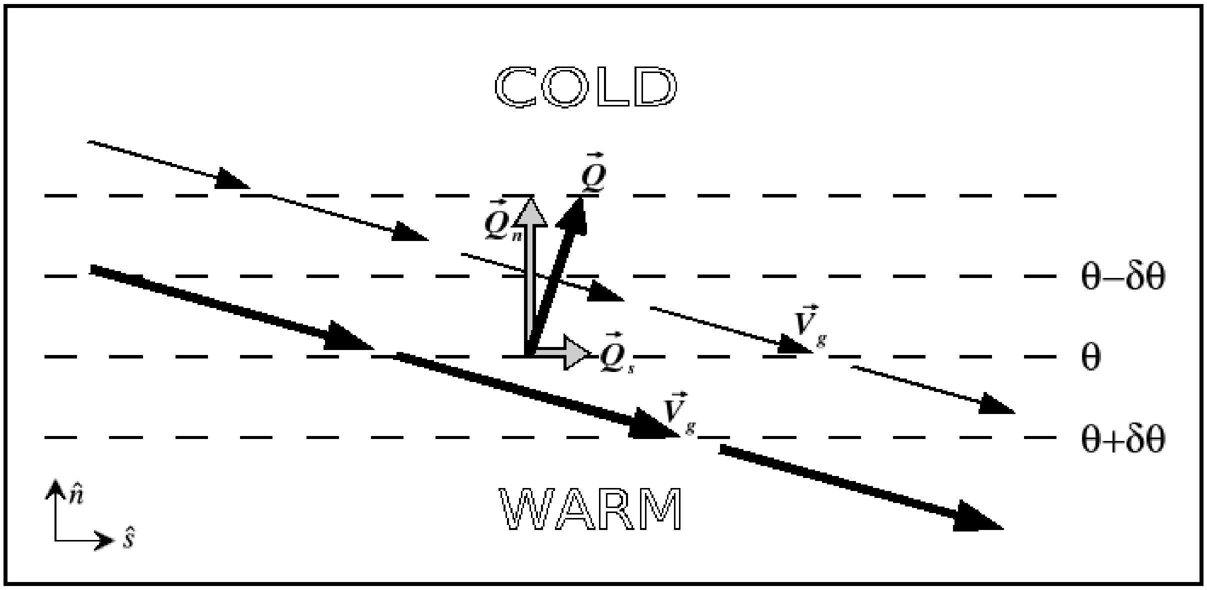

Figure 2.3: A schematic depiction of cold air advection in a region of cyclonic shear on an isobaric surface from the ***Q****-vector perspective. The geostrophic winds are represented by the arrows labeled* $\vec{V}_g$ *, the dashed lines represent the isentropes.*

three-dimensional vector forcing functions. They examined developing upper-fronts in both northwesterly and southwesterly flow, paying particular attention to the contributions of vertical tilting in both scalar and rotational frontogenesis. For their northwesterly flow case, they observed that the contributions of vertical titling to scalar frontogenesis throughout the life-cycle of the upper-front were consistently frontogenetic. They also noted that the observed vertical tilting contributing to rotational frontogenesis consistently favored a negative, anticyclonic rotation of the isentropes. However, the observed rotation of the isentropes in their analysis was cyclonic, which suggested to them that the dominant forcing for rotational frontogenesis derived not from vertical tilting, but from the horizontal terms, particularly the contributions of vorticity. In their analysis, they noted that the largest region of positive rotational frontogenesis was observed along the vorticity maximum found within a developing upper-front. The observed positive rotational frontogenesis resulted in a cyclonic rotation of the isentropes, which initiated cold air advection along the front. In a region of cyclonic shear, this cold air advection would favor the production of a thermally indirect vertical circulation and further intensification of the upper-front via vertical tilting.

Schultz and Doswell (1999) established that rotation of the isentropes was an important precursor for establishing regions of cold air advection along an upper-front. They provided an updated conceptual model of the evolution of an upper-front in northwesterly flow over North America, based upon Shapiro's pioneering conceptual model (1982; his Fig. 7, here Fig. 1.4), by focusing on the important *cold-advection stage* of development (Fig. 2.4). From their observational study, they suggested that the initial cold air advection along the length of the upper-front would become concentrated at the base of the thermal trough, a consequence of the developing vorticity maximum and its effect on rotational frontogenesis and the thermal field during the early stages of the upper-front development. In fact, they noted that weak cold or even warm advection was observed in the northwest extension of the front, upstream of the thermal trough. In contrast with the Shapiro (1982) model, which depicted pervasive cold air advection along the length of the front, the Schultz and Doswell (1999) model captured the differential thermal advection that formed along the length of the developing upper-front. They also suggested that the strongest cold air advection developed in conjunction with an intensifying and compacting vorticity maximum, an aspect of upper frontogenesis neglected in the Shapiro model. The development of cold air advection produced strong frontogenetic tilting and the development of an intense upper-front. However, since they developed an extension of (2.2), (which included the full wind, not the

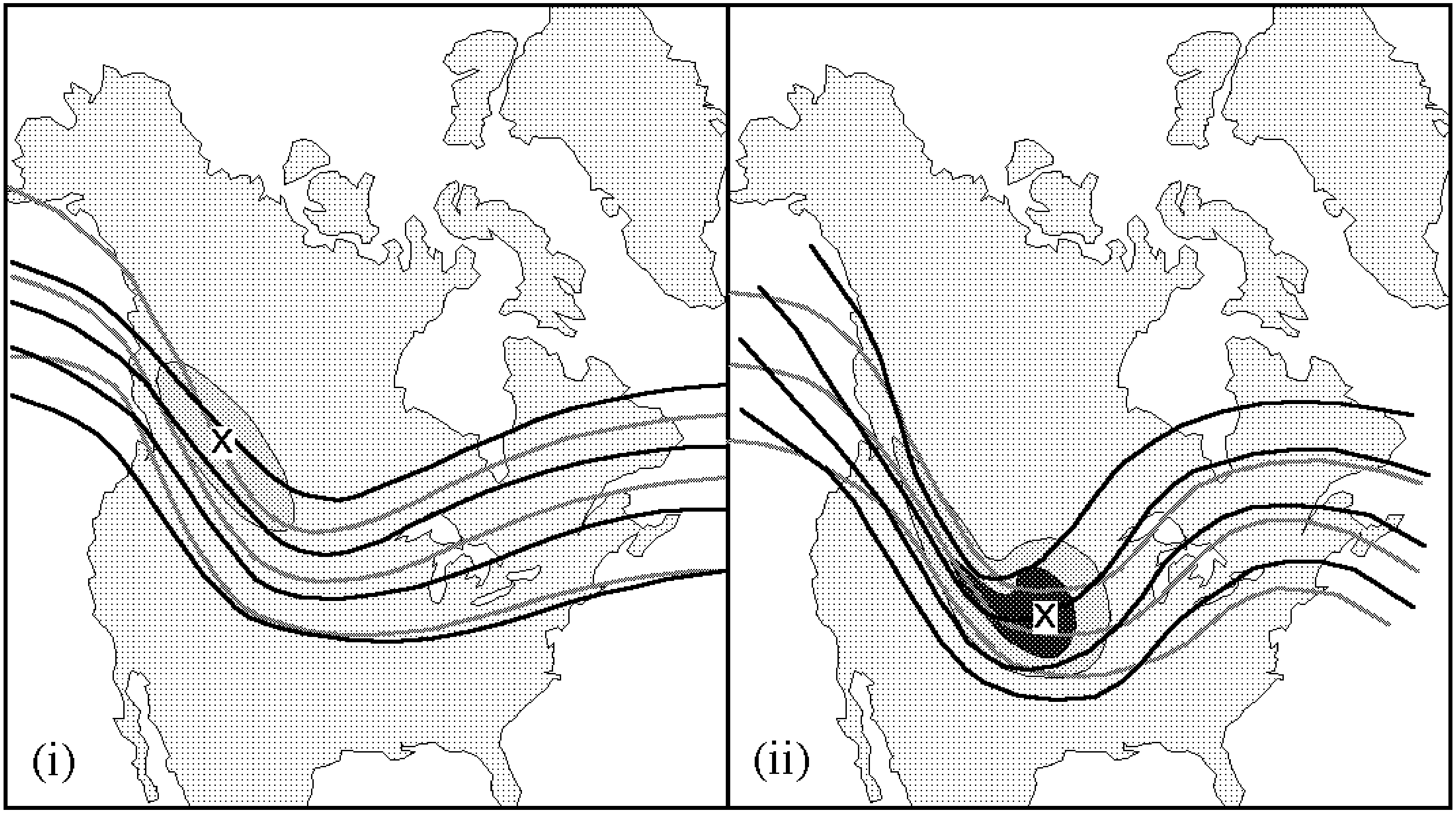

Figure 2.4: The Schultz and Doswell revised conceptual model, on an isobaric surface, of the early development of an idealized upper-level jet-front system in the northwesterly flow of a mid-latitude baroclinic wave over a 12-24 hour period. The light gray lines represent geopotential height contours, the solid black lines represent isentropes, the shaded regions represent positive absolute vorticity with a local maximum at X. *(i) Early development of the upper-jet front system, geostrophic cold air advection implied along the length of the front. (ii) Geostrophic cold air advection concentrated at the base of the trough, upper-level jet-front and vorticity maximum increase concurrently. From Schultz and Doswell (1999, their Fig. 16b).*

geostrophic wind) they were not able to isolate the vertical motions associated with the rotational frontogenesis that spawned the initiation of the important along-front cold air advection. Without the quantification of these associated vertical motions, a potentially important feedback within the upper frontogenesis process remains unexplained.

In this research, we employ a QG frontogenesis perspective, rooted in the components of the partitioned $\vec{Q}$ vector, in order to explicitly examine the distribution of both the shearwise (ω_s) and transverse (ω_n) vertical motions throughout the life-cycle of a robust upper-level front. Of particular interest is the evolution of the shearwise vertical motion field, as it is directly associated with the important QG rotational frontogenesis. Through examination of the evolving distribution of the shearwise vertical motion during the life-cycle of an intense upper-level front, we will isolate the vertical motion associated with the rotational frontogenesis and thereby develop a more complete understanding of the role of rotational frontogenesis in the development of upper-level frontal zones.

3. Case Overview

During the second week of November 2003, a high amplitude flow developed over North America, with the polar jet dipping southward from 60°N to roughly 40°N along the west coast of North America, while the sub-tropical jet sliced northeastward from well off the coast of southern California to Michigan. The northwesterly flow along the northwest coast was characterized by a region of strong baroclinicity that subsequently evolved into a potent upper-front over the next two days. During this period, the temperature gradient characterizing the front intensified as the feature migrated through northwesterly flow, rounded the base of a geopotential height trough, and finally emerged in southwesterly flow. During this evolution, the front traveled from the Alaskan Peninsula to the Midwest and eventually became a precursor to a substantial continental cyclongenesis event described by Martin (2006).

The high amplitude flow pattern over North America at 0000 UTC 11 November is shown in Fig 3.1. The 500 hPa northwesterly flow over the Gulf of Alaska was characterized by a rather weak baroclinic zone at this time, with a potential temperature gradient of 2.25 K per 100 km (Fig. 3.1a). Embedded in this baroclinic zone were several patches of enhanced vorticity located over the Gulf of Alaska and the British Colombia coast. In the region where the northwesterly flow entered the northwest United States, the baroclinic zone was weaker. Another noteworthy feature at 500 hPa was the dominant positively tilted shortwave trough that stretched southwestward from southern Nevada, across the California coast into the Pacific Ocean. The upper-level flow over the United States was characterized by a second

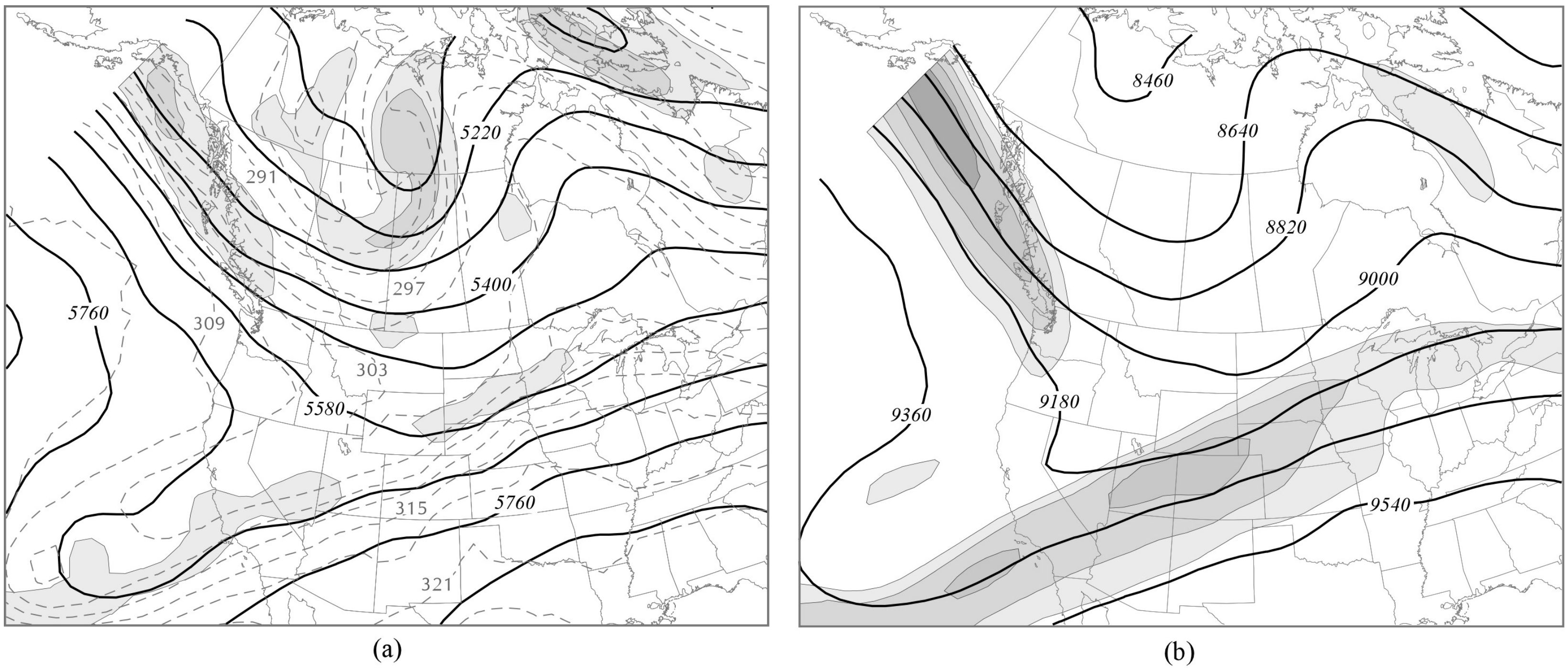

Figure 3.1: From the 0-hour forecast of the NCEP Eta model valid at 0000 UTC 11 November 2003, (a) the 500 hPa geopotential height (solid lines) in meters, potential temperature (dashed lines) in K, and absolute vorticity (shaded) every $5x10^{-5}$ s^{-1}, beginning at $15x10^{-5}$ s^{-1}. (b) The 300 hPa geopotential height (solid lines) in meters and magnitude of the wind (shaded) every 10 m s^{-1}, beginning at 40 m s^{-1}.

baroclinic zone that originated downstream of the axis of this shortwave and stretched northeastward over the Rockies to the Upper Midwest (Fig 3.1a). These two regions of baroclinicity were coincident with the locations of the polar and subtropical jets at this time (Fig. 3.1b). The polar jet was fairly linear with a maximum of over 70 m s^{-1} located in the Gulf of Alaska. Likewise, the jet associated with the subtropical flow was linear and exhibited two maxima of over 60 m s^{-1}; one off the southern California coast and the other over the Utah-Colorado Rockies.

By 1200 UTC 11 November, the strongly baroclinic northwesterly flow entered the northwest United States (Fig. 3.2a). This baroclinic zone contained a strip of vorticity oriented along the isentropes from extreme southeastern Alaska to Washington. Downstream of the Pacific Northwest, the baroclinic zone weakened. Downstream of the axis of the southern shortwave, the second region of baroclinicity extended into the Great Lakes region (Fig. 3.2a). The jet associated with this shortwave and the sub-tropical flow was linear with one maximum of over 70 m s^{-1} found over the central Plains (Fig. 3.2b). In the intervening twelve hours, the polar jet moved further to the southeast, was oriented nearly perpendicular to the subtropical jet, and was also a fairly linear feature with a maximum speed of 70 m s^{-1} over southeast Alaska (Fig. 3.2b).

By 0000 UTC 12 November (Fig. 3.3), the northern 500 hPa shortwave, located at the left exit region of the polar jet, had shifted slightly eastward as had its associated baroclinic zone (Fig. 3.3a). The southern extremity of this developing upper-front reached further south than at the previous time, extending into southwestern Wyoming. Here the warm side of the upper-front ingested the 306 and 309 K isentropes, that had been associated with the cold

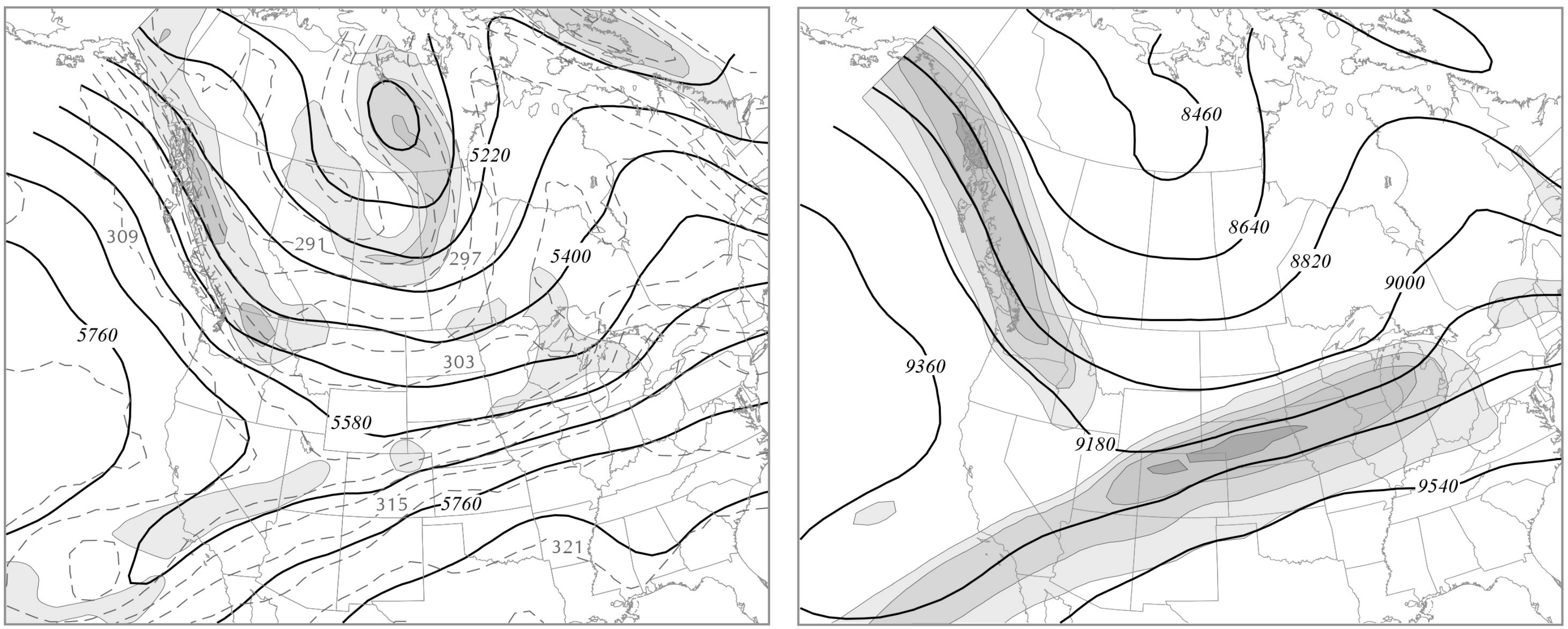

(a) (b)

Figure 3.2: As Fig. 3.1, but for 1200 UTC 11 November 2003.

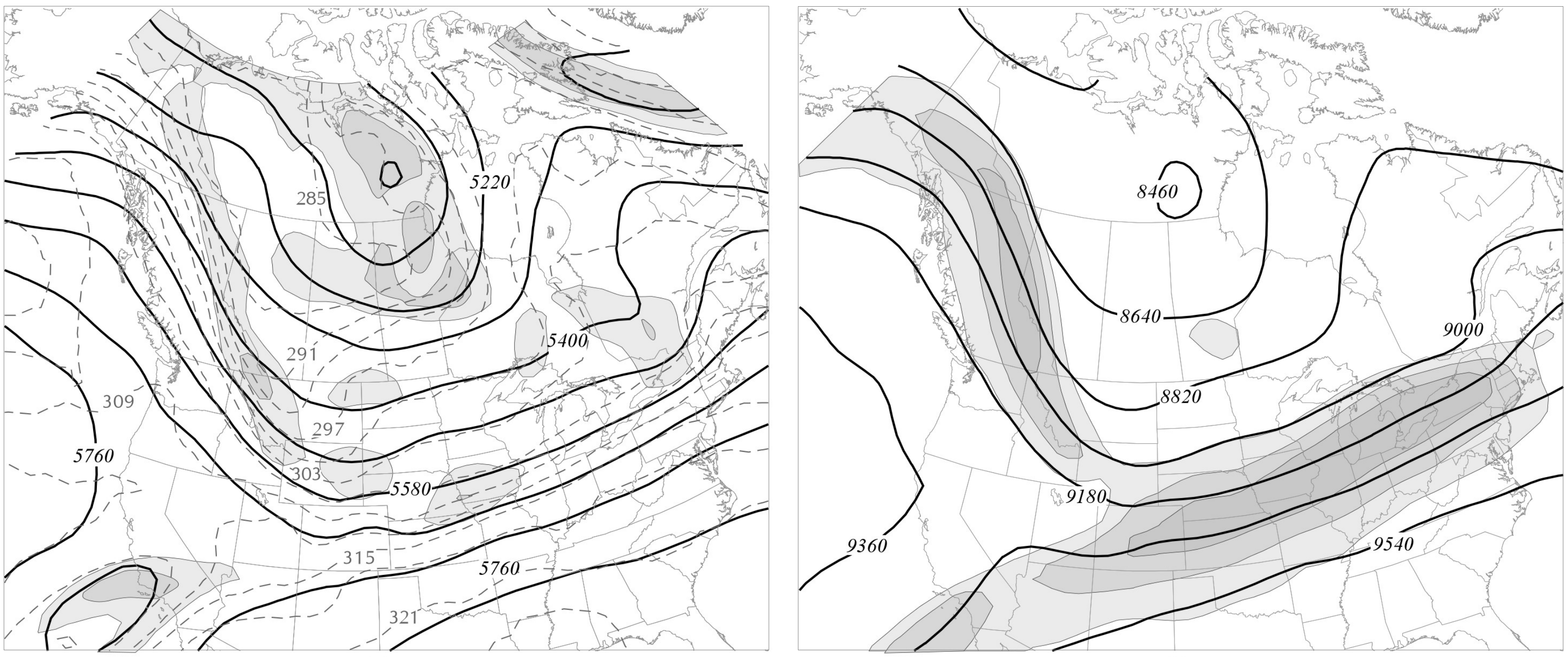

(a) (b)

Figure 3.3: As Fig. 3.1, but for 0000 UTC 12 November 2003.

side of the baroclinic zone in southwesterly flow at the previous time. The amplification of the 500 hPa thermal trough was also significant by this time, with its axis stretching from central Alberta, through western Montana, into Wyoming. The magnitude of the absolute vorticity positioned along the upper-front had not changed significantly in the intervening twelve hours (Fig. 3.3a). At 300 hPa the northwesterly jet axis was also oriented more or less along the isentropes that defined the upper-front. The maximum wind speed, centered over the British Columbia-Alberta border, had decreased to just over 60 m s^{-1} (Fig. 3.3b). This jet exhibited an abrupt exit region, situated near the Idaho-Wyoming border, where the flow joined the northern edge of the southwesterly sub-tropical jet along the front range of the Rocky Mountains.

By 0600 UTC 12 November (Fig. 3.4), the developing upper-front stretched from the ridge over the Yukon-Northwest Territories border to the axis of the shortwave trough along the Wyoming-Nebraska border (Fig. 3.4a). The strongest section of the upper-front, defined by the maximum temperature gradient, was located in western Montana and Wyoming, slightly upstream of the trough axis and near the maximum in 500 hPa vorticity. Upstream of this intense section of the upper-front, the 60 m s^{-1} maximum wind in the northerly jet streak was positioned over central Alberta, approximately at the inflection point in the baroclinic ridge-trough system (Fig. 3.4b). The flow exited this jet streak and entered the southwesterly jet that reached from the southern California coast to well east of the Great Lakes region. The 60 m s^{-1} maximum winds of this southern jet covered an expansive area from the lee of the Rockies to east of the Great Lakes.

At 1200 UTC 12 November (Fig. 3.5), the intensity of the upper-level front increased

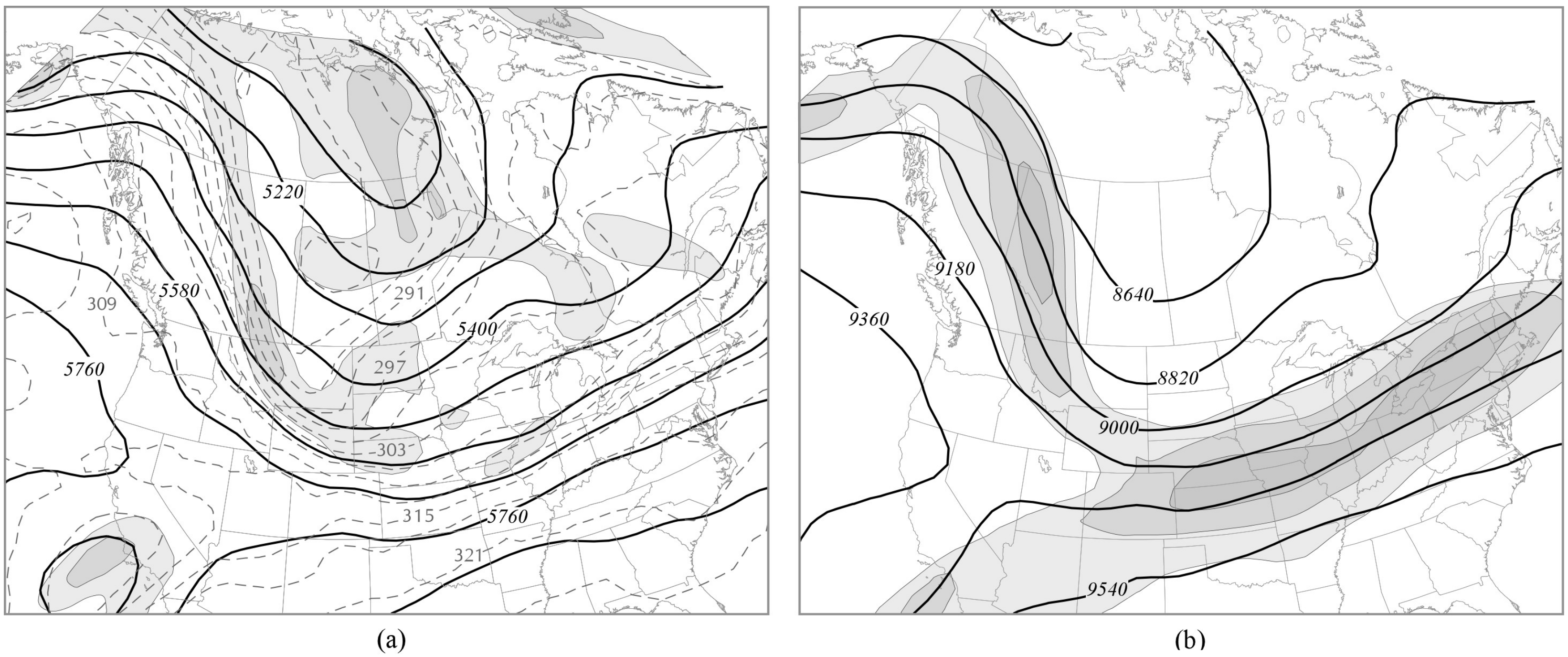

Figure 3.4: As Fig. 3.1, but for 0600 UTC 12 November 2003.

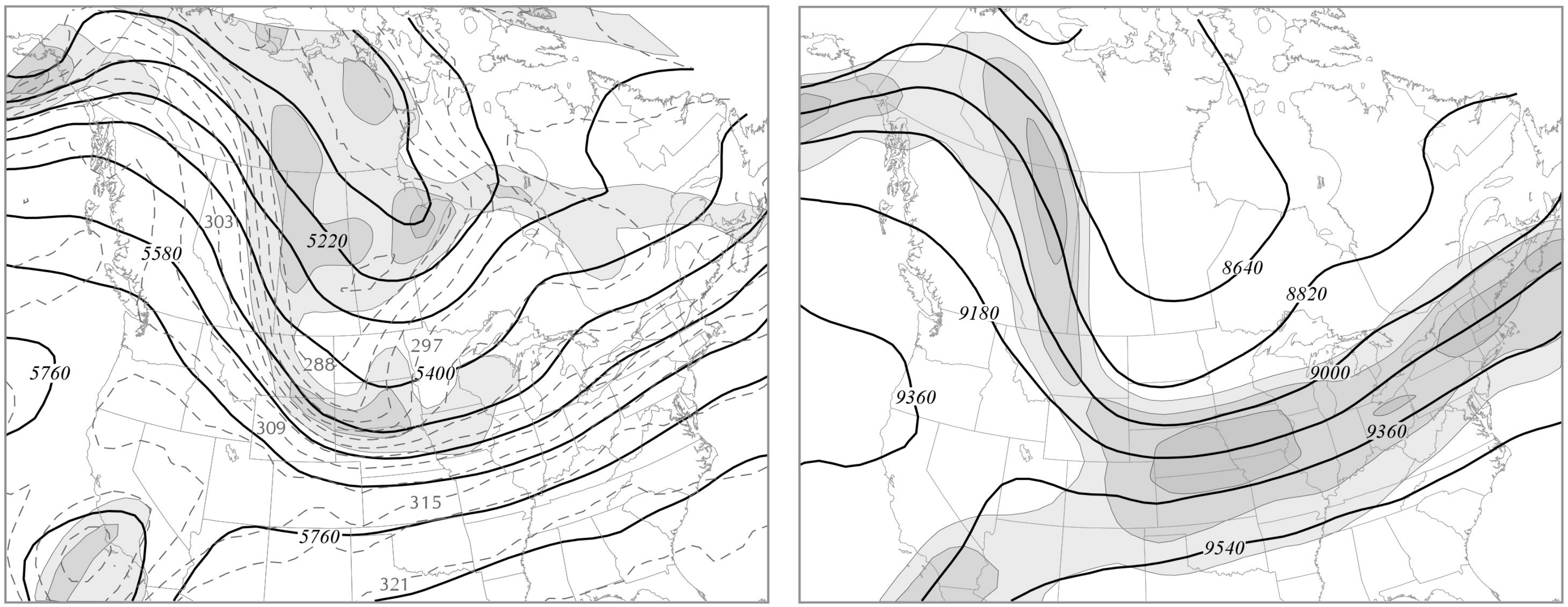

(a) (b)

Figure 3.5: As Fig. 3.1, but for 1200 UTC 12 November 2003.

from Alberta southward into the upper Plains of the United States where it reached the base of the geopotential height trough over eastern Nebraska. The strongest portion of the front was centered on the eastern border of Wyoming, where the potential temperature gradient was approximately 5.25 K per 100 km (Fig. 3.5a). The absolute vorticity maxima was co-located with this portion of the front (Fig. 3.5a). At 300 hPa, the abrupt exit region of the northwesterly jet weakened. The flow joined the southwesterly jet streak, creating a meandering polar jet which had several speed maxima of over 60 m s^{-1} scattered across northern Alberta, the central Plains, and the southern Great Lakes regions (Fig. 3.5b).

By 1800 UTC 12 November (Fig. 3.6), the upper-front continued its progression though the base of the shortwave trough over the central Plains. The absolute vorticity and the most intense segment of the upper-front were located within the base of this trough and stretched from eastern Montana through Nebraska and eastward into Iowa (Fig. 3.6a). The development of a small shortwave contributed to the enhancement of the local maximum in vorticity slightly upstream of the trough axis. At 300 hPa, the northerly jet centered over northwestern Saskatchewan was sustained at 60 m s^{-1} (Fig. 3.6b). However, the jet maximum situated over the Plains had become the dominant jet feature. It intensified to a magnitude of over 70 m s^{-1} centered over central Iowa and was characterized by weak geostrophic cold air advection, as implied by the orientation of the geopotential height contours and isentropes in Fig. 3.6a.

By 0000 UTC 13 November (Fig. 3.7), the intense upper-front stretched from the northern Plains to the Great Lakes region where the front emerged in the southwesterly flow over lower Michigan (Fig. 3.7a). The magnitude of the potential temperature gradient was

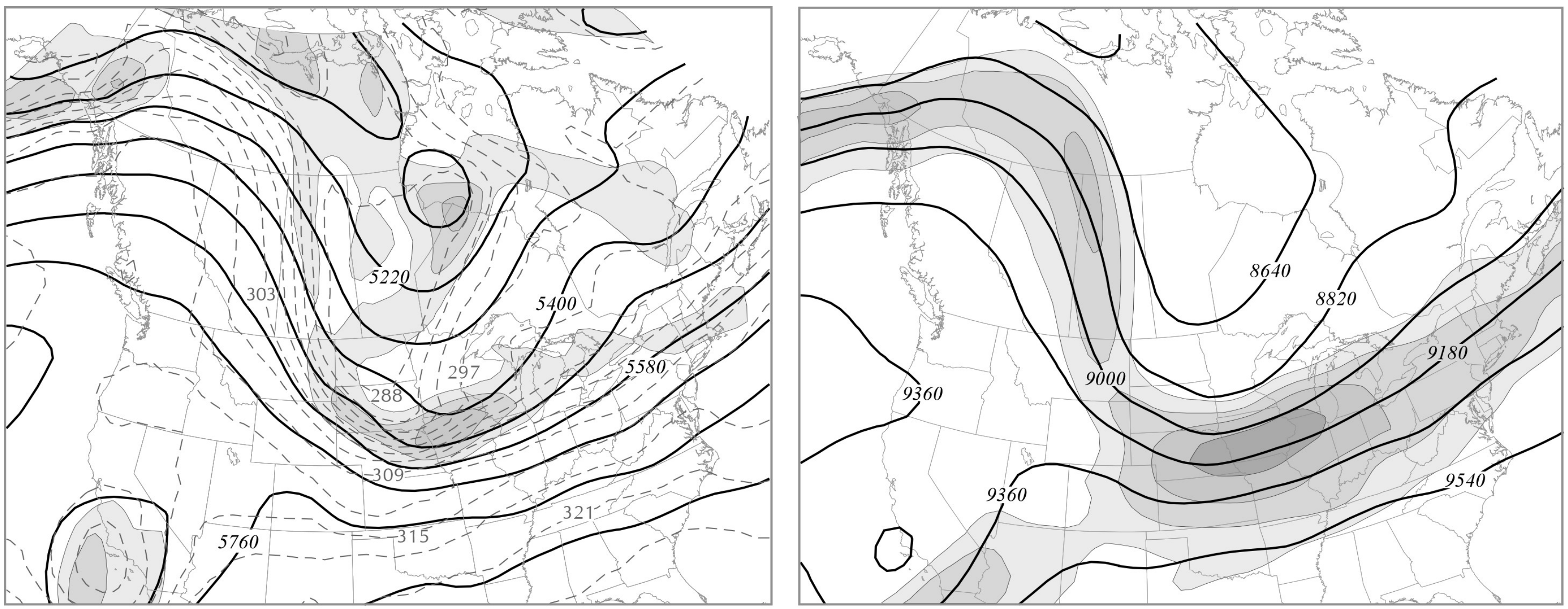

(a) (b)

Figure 3.6: As Fig. 3.1, but for 1800 UTC 12 November 2003.

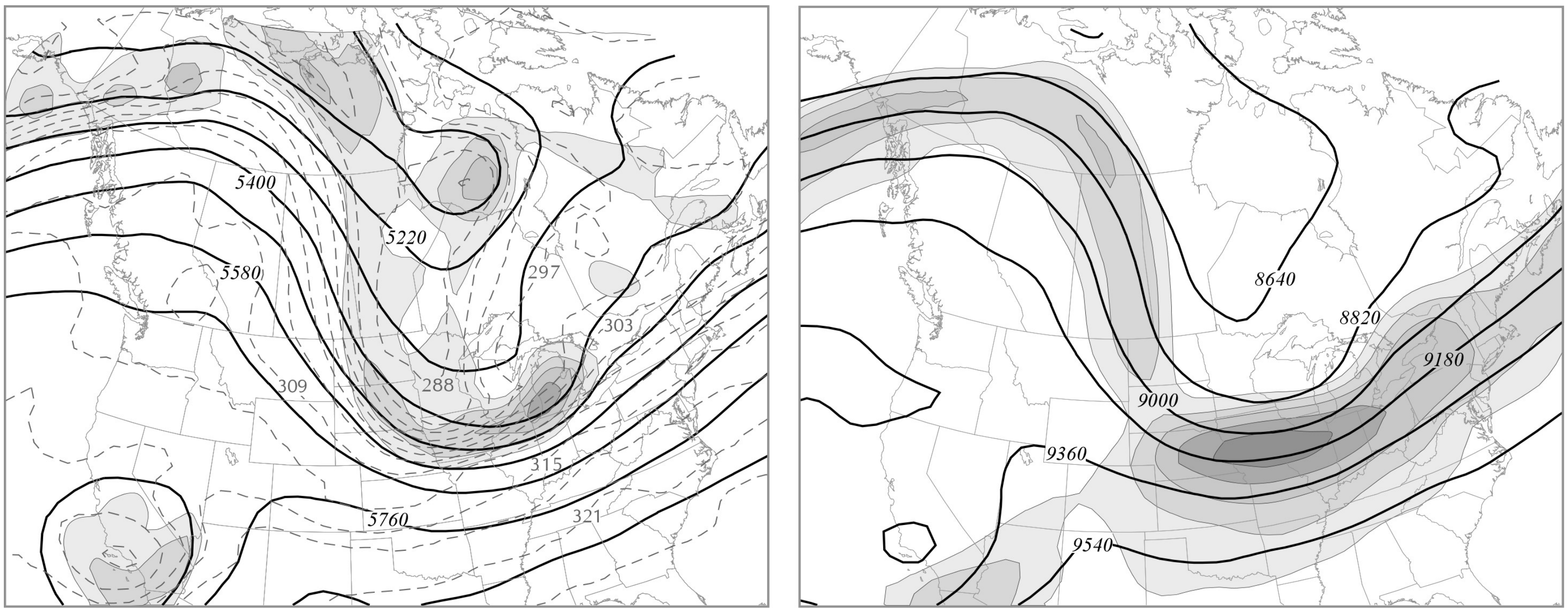

(a) (b)

Fig. 3.7: As Fig. 3.1, but for 0000 UTC 13 November 2003.

also the strongest at this time, approximately 8 K per 100 km in central Iowa. The absolute vorticity at 500 hPa was oriented in a strip along the upper-front, with a local maximum at its eastern edge of the frontal zone (Fig. 3.7a). The 300 hPa jet streak centered over southern Iowa continued to intensify, reaching speeds of over 80 m s^{-1} (Fig 3.7b). The jet axis was oriented along the warm side of the upper-front with increased geostrophic cold air advection through the jet core, implied, as before, in Fig. 3.7a. After this time, the upper-front became a component of a troposphere-deep frontal structure associated with the cyclogenesis event described by Martin (2006).

4. Quasi-Geostrophic Vertical Motion

In the subsequent analysis, gridded model output from the National Centers for Environmental Prediction's (NCEP's) Eta and Global Forecast System (GFS) models is used in the calculation of QG omega and its components. These gridded data are first bilinearly interpolated from their original output grid to a 1°x1° latitude–longitude grid at 19 isobaric levels (1000, 950, 900, 850, 800, 750, 700, 650, 600, 550, 500, 450, 400, 350, 300, 250, 200, 150, and 100 hPa) using an interpolation program included in the General Meteorological Analysis Package (GEMPAK). Employing the technique of successive over relaxation (SOR), we then solve the *f*-plane version of the QG omega equation using a spatially averaged static stability that varies for each time with f_o set equal to the central latitude (45.5°N) of the domain for this case. With geostrophic forcing corresponding to the divergences of $\boldsymbol{Q}$, $\boldsymbol{Q}_n$, and $\boldsymbol{Q}_s$, the total, transverse, and shearwise QG vertical motions, respectively, are returned in units of Pa s^{-1}. In this section, the evolution of QG omega will be examined at both the 500 hPa level and in vertical cross sections corresponding to the time periods analyzed in the *Synoptic Overview* section. The 500 hPa level is chosen for this analysis as it is, in the literature, the most commonly referenced isobaric level for describing the vertical motions associated with the development of upper-fronts. The thermal structures at 500 hPa at 1200 UTC 11 November, 0000 UTC 12 November, and 1800 UTC 12 November, were also used to select the vertical cross sections of interest.

The 500 hPa total QG vertical motion field at 0000 UTC 11 November 2003 is shown in Fig. 4.1a. The baroclinic zones in both the northwesterly and southwesterly flow were populated by multiple couplets of ascent and descent, the majority of which were oriented along the isentropes. Within the northwesterly flow, a dominant couplet of vertical motion was positioned at the southern extent of the baroclinic zone over British Columbia, with the isentropes becoming diffluent immediately downstream of the ascent. As might be expected by the orientation of the omega couplets, almost all of the vertical motion found along the two baroclinic zones was captured by shearwise omega (Fig 4.1b). In the northwesterly flow, the shearwise subsidence was positioned so that it was maximized on the warm side of the baroclinic zone over the Queen Charlotte Islands. At this early time in the development of the upper-front, only a small patch of transverse ascent in the northwesterly flow (Fig. 4.1c) contributed to the total QG vertical motion. The relatively strong couplet of shearwise vertical motion along the British Columbia coast suggests that the QG rotational frontogenesis was active and promoting a counterclockwise rotation of the isentropes in this region.

At 1200 UTC 11 November, the northwesterly flow baroclinic zone was characterized by several pockets of subsidence along the Canadian west coast (Fig 4.2a). At the southern end of the baroclinic zone, ascent was located from eastern Washington to southern Alberta and the isentropes became diffluent immediately downstream of this region. In the partitioned omega fields, pockets of shearwise omega continued to capture nearly all of the full QG vertical motion in the northwesterly flow (Fig. 4.2b). Transverse omega contributed very little to the full QG omega in the vicinity of the upper-front (Fig. 4.2c).

Several cross sections were constructed at 1200 UTC 11 November, each

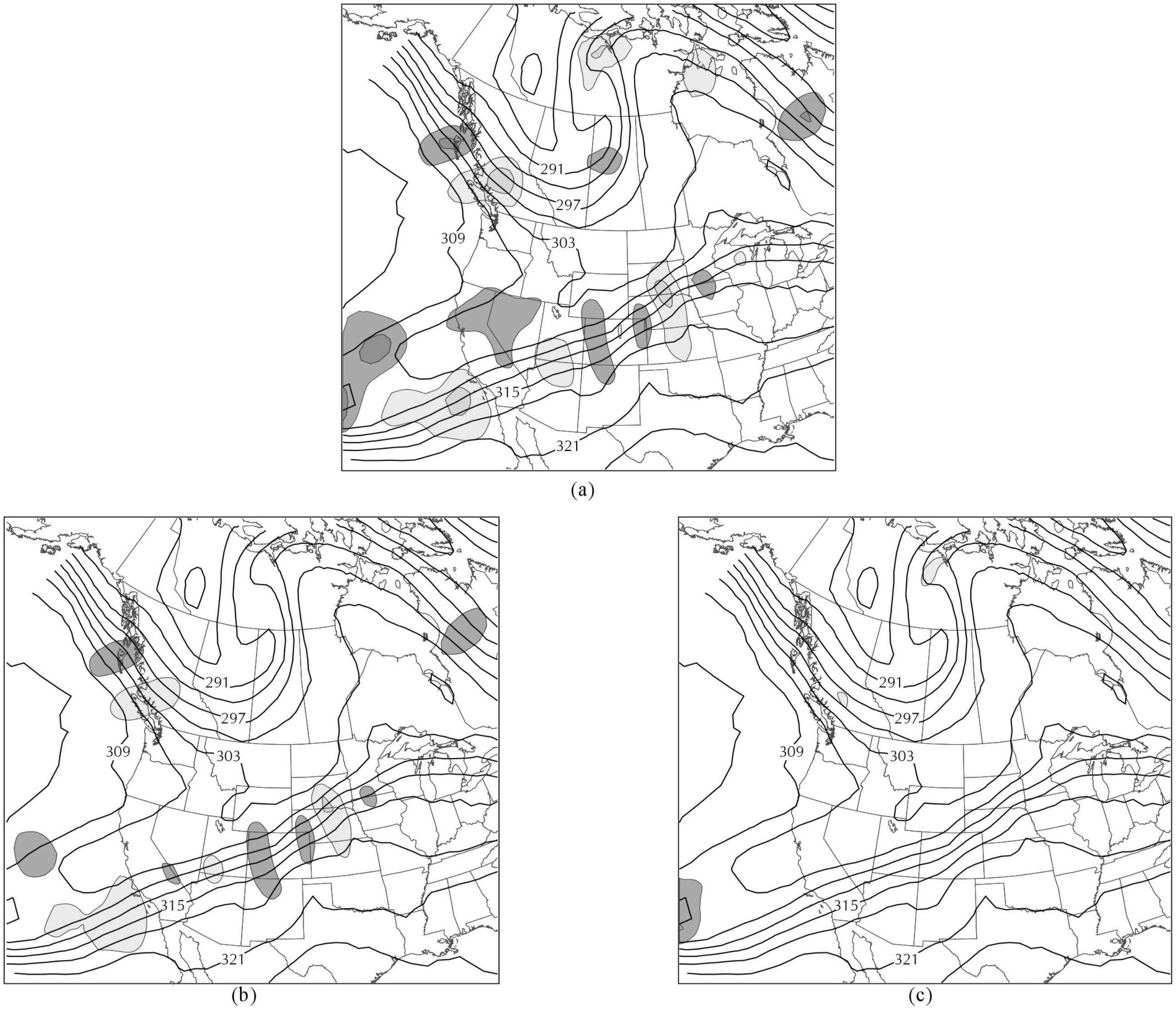

*Figure 4.1: Valid at 0000 UTC 11 November 2003, the 500 hPa isentropes (solid lines) and (a) the total QG vertical motion associated with the full **Q**-vector, (b) the shearwise QG vertical motion, ω_s, associated with rotational frontogenesis, $\mathbf{Q}_s$, and (c) the transverse QG vertical motion, ω_n, associated with scalar frontogenesis, $\mathbf{Q}_n$, every 2 dPa s^{-1} with dark (light) shading corresponding to descent (ascent).*

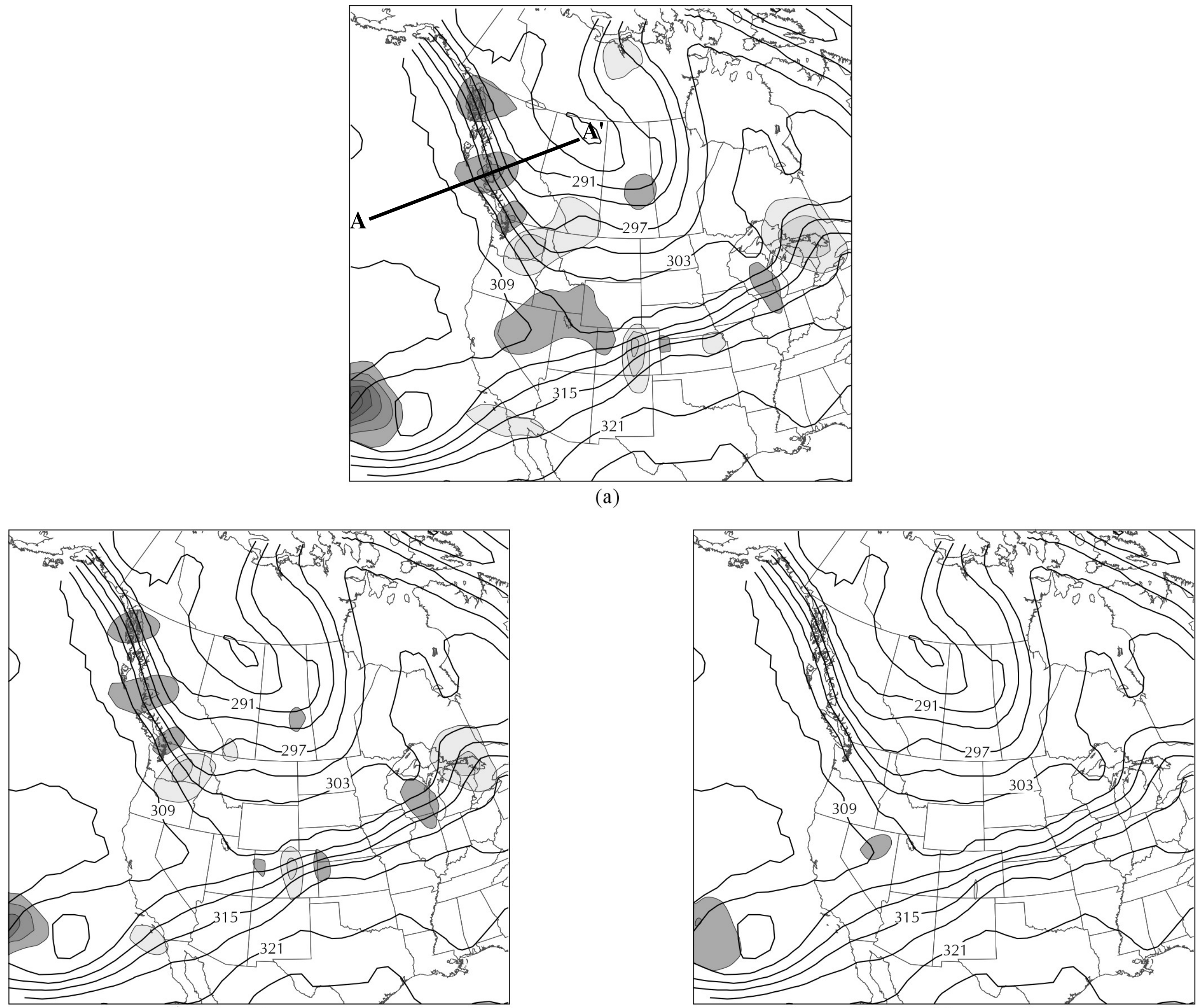

Figure 4.2: As Fig. 4.1, but for 1200 UTC 11 November 2003.

perpendicular to the isentropes that defined the upper-front along the line A-A', in Fig. 4.2a. The total QG omega along this cross section, illustrated in Fig. 4.3a, shows subsidence between 325 hPa and 800 hPa with a maximum centered at approximately 475 hPa, on the warm side the baroclinic zone beneath the jet core. Nearly all of the differential subsidence across the baroclinic zone was accounted for by the shearwise component of vertical motion (Fig. 4.3b), as the transverse vertical motion contributed next to nothing to the differential subsidence across the front (Fig. 4.3c). The shearwise subsidence, forced by QG rotational frontogenesis, was positioned directly beneath the jet core. This orientation provided the necessary subsidence that promoted an increase the magnitude of the potential temperature gradient in this region.

At 0000 UTC 12 November, subsidence continued to dominate the total QG vertical motion in the northwesterly flow as the upper-front intensified (Fig 4.4a). The southern extent of the frontal zone, located in southwest Wyoming, was characterized by the largest subsidence with two local maxima on the warm side of the front. Examining the shearwise omega field (Fig. 4.4b) revealed that it did not fully capture the subsidence in the southern region of the frontal zone, as it had at previous times (Fig. 4.2b). The segment of the upper-front with the largest horizontal temperature gradient, along the Idaho-Montana border, was also characterized by the greatest shearwise subsidence. While shearwise omega contributed the majority of the subsidence, the transverse component of QG omega played a larger role in forcing warm side subsidence than it had at any of the previous times (Fig. 4.4c). Interestingly, this subsidence was found in the exit region of the northwesterly jet streak, where a thermally indirect transverse circulation should occur. However, the correspondingly

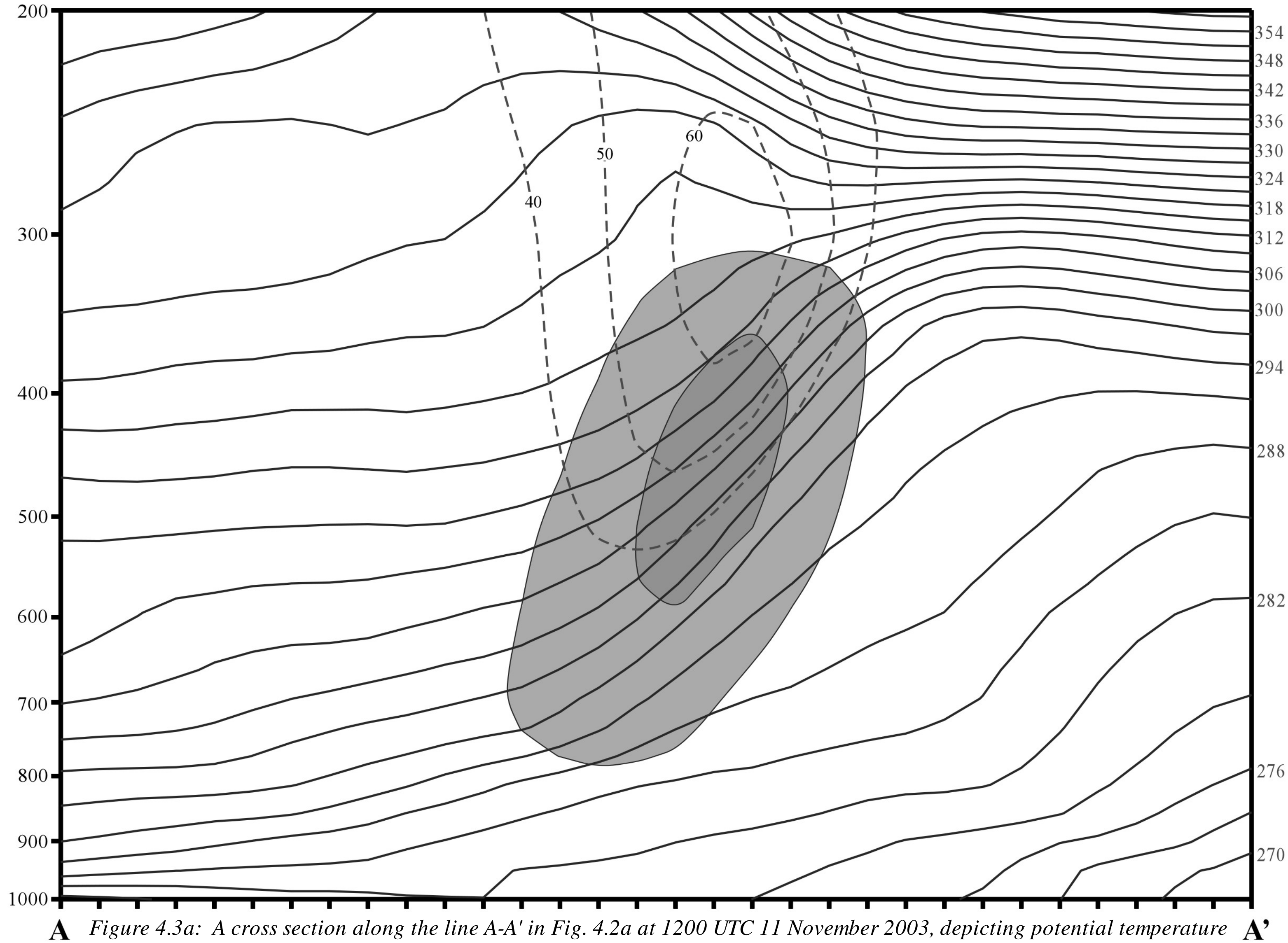

Figure 4.3a: A cross section along the line A-A' in Fig. 4.2a at 1200 UTC 11 November 2003, depicting potential temperature (solid lines) every 3 K, isotachs (dashed lines) every 10 m s^{-1} beginning at 40 m s^{-1}, and total QG vertical motion every 2 dPa s^{-1}, beginning at 2 dPa s^{-1}.

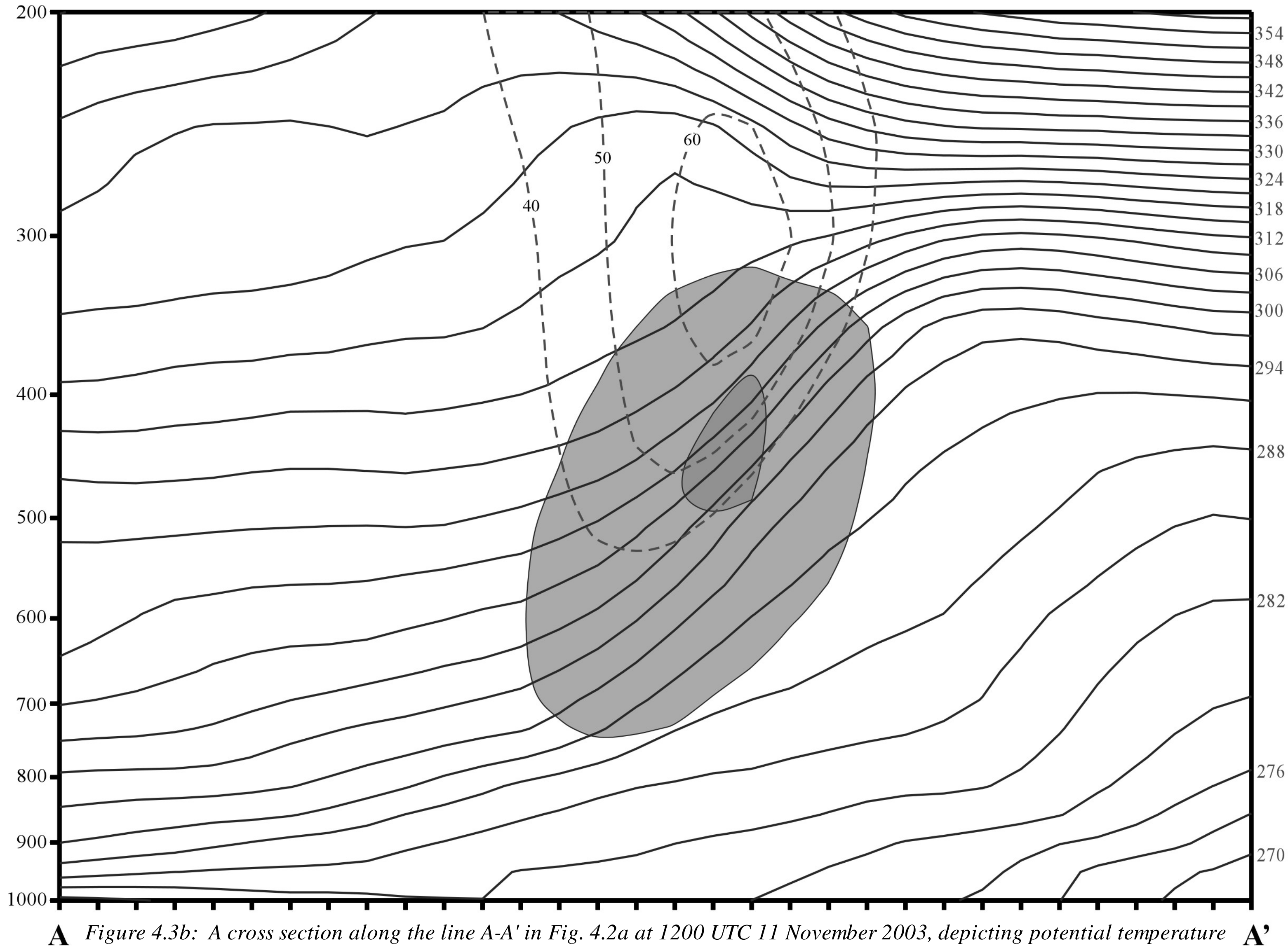

Figure 4.3b: A cross section along the line A-A' in Fig. 4.2a at 1200 UTC 11 November 2003, depicting potential temperature (solid lines) every 3 K, isotachs (dashed lines) every 10 m s^{-1} beginning at 40 m s^{-1}, and shearwise QG vertical motion every 2 dPa s^{-1}, beginning at 2 dPa s^{-1}.

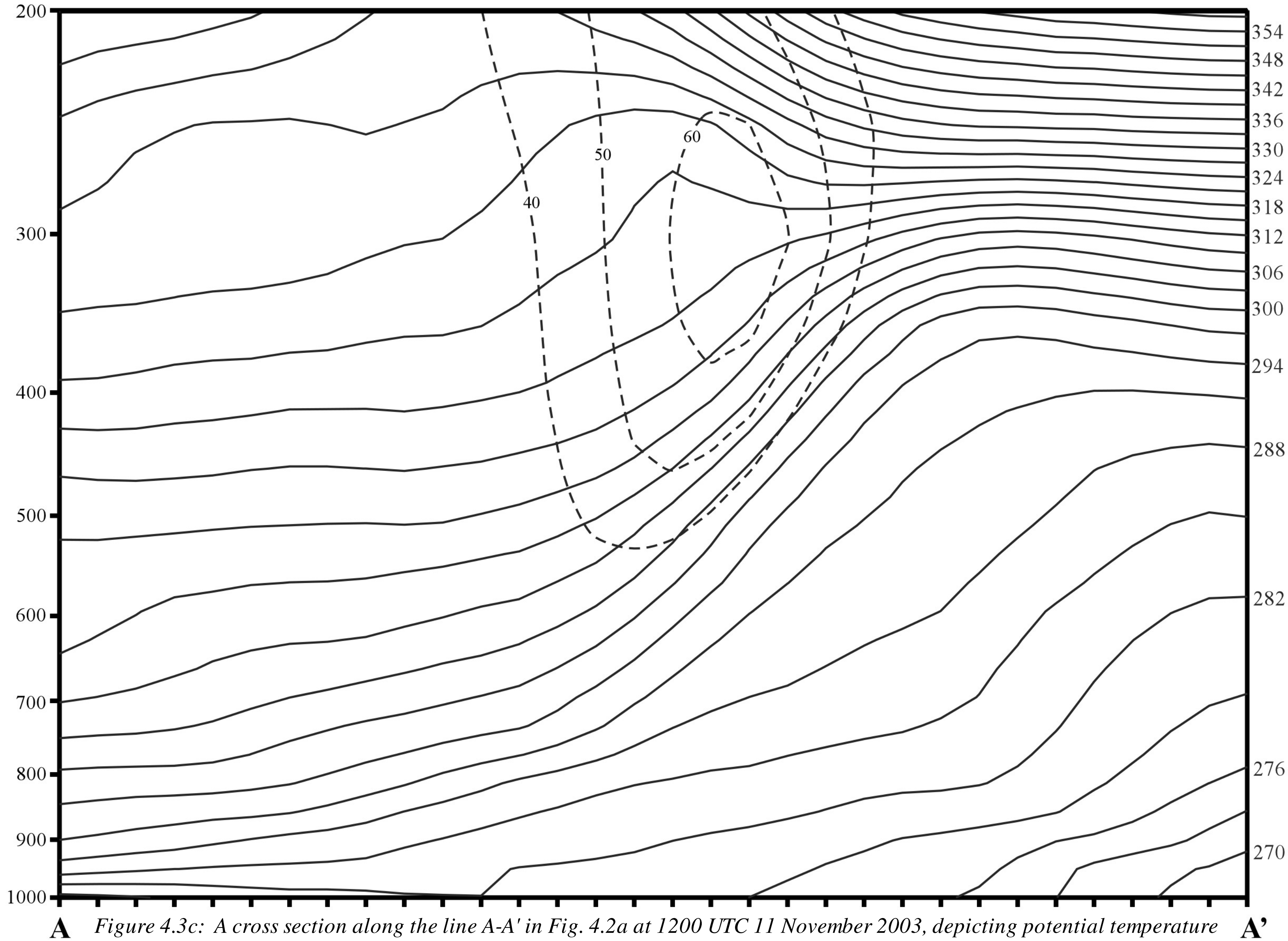

Figure 4.3c: A cross section along the line A-A' in Fig. 4.2a at 1200 UTC 11 November 2003, depicting potential temperature (solid lines) every 3 K, isotachs (dashed lines) every 10 m s^{-1} beginning at 40 m s^{-1}, and transverse QG vertical motion every 2 dPa s^{-1}, beginning at 2 dPa s^{-1}.

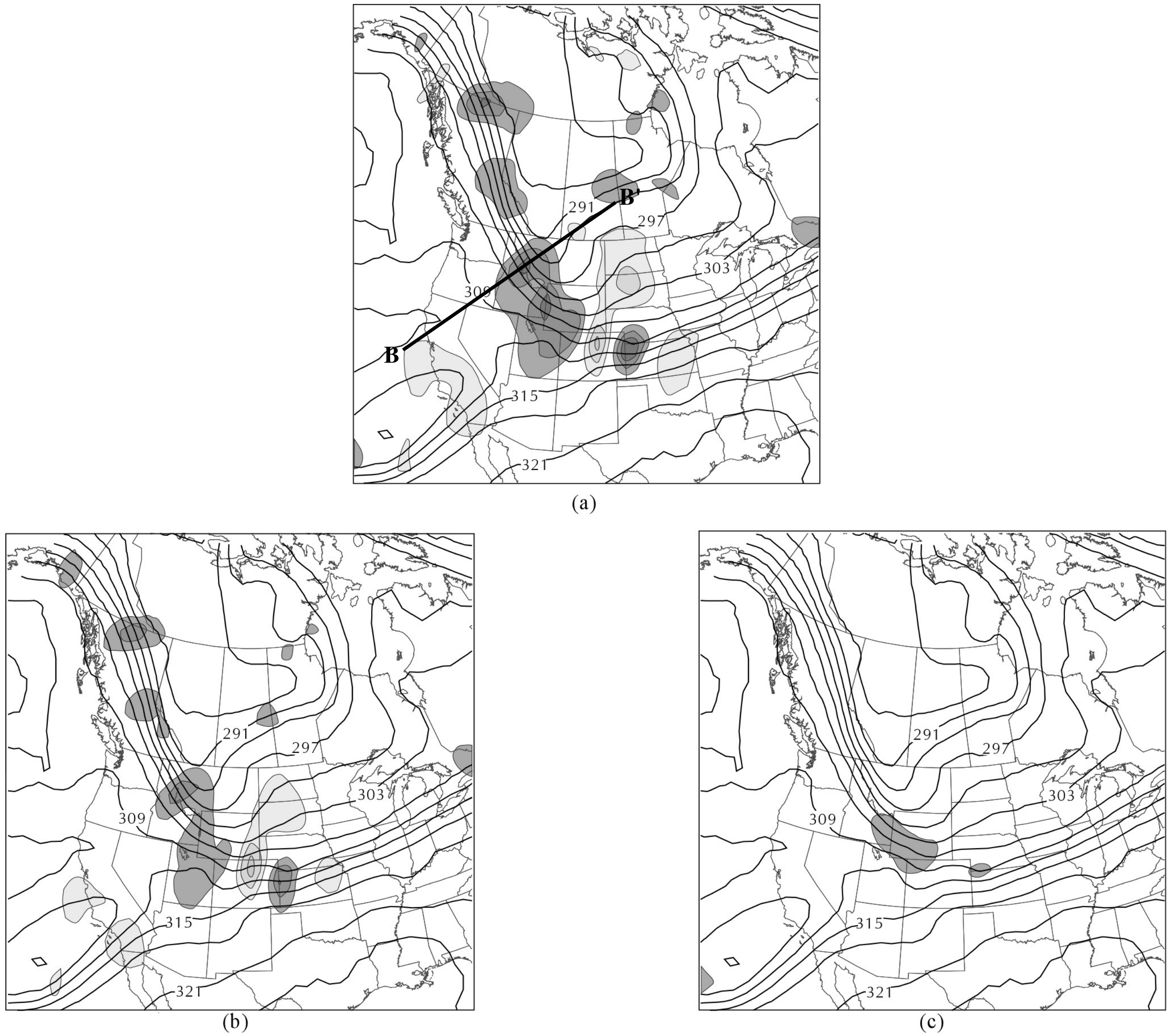

Figure 4.4: As Fig. 4.1, but for 0000 UTC 12 November 2003.

weak transverse ascent, which should be in the left exit region of the jet streak, was apparently diluted by curvature in the flow which induced weak descent.

Several vertical cross sections were constructed at 0000 UTC 12 November along the line B-B' in Fig. 4.4a, through the northern region of maximum subsidence within the upper frontal zone. QG subsidence characterized the entire depth of the troposphere above and below the upper-front, but beneath the jet core, with a local maximum between 600 to 300 hPa (Fig. 4.5a). The 303 K isentrope sloped from approximately 300 hPa to 700 hPa across the front from north to south, representing the path along which stratospheric air might be extruded deep into the troposphere. Shearwise omega was responsible for the majority of the subsidence throughout the depth of the troposphere (Fig. 4.5b). However, the small patch of transverse subsidence located on the warm side of the upper-front, with a maximum centered at approximately 400 hPa, was in a position where it too contributed to the thermally indirect circulation that promoted upper frontogenesis.

At 0600 UTC 12 November, the pockets of QG subsidence throughout the northwesterly flow continued to amplify along the intensifying upper-front (Fig. 4.6a). The strongest subsidence, with a magnitude of 10 dPa s^{-1}, was located along the southernmost section of the frontal zone in northwestern Wyoming. This location also marked the maximum in shearwise subsidence, approximately 6 dPa s^{-1}, which was the largest component of the total QG vertical motion (Fig. 4.6b). The shearwise vertical motion accounted for nearly all of the subsidence in the baroclinic zone, upstream of the local maximum. The contribution of the transverse subsidence continued to increase, with a linear band of subsidence oriented within and towards the warm side of the upper-front in Wyoming (Fig.

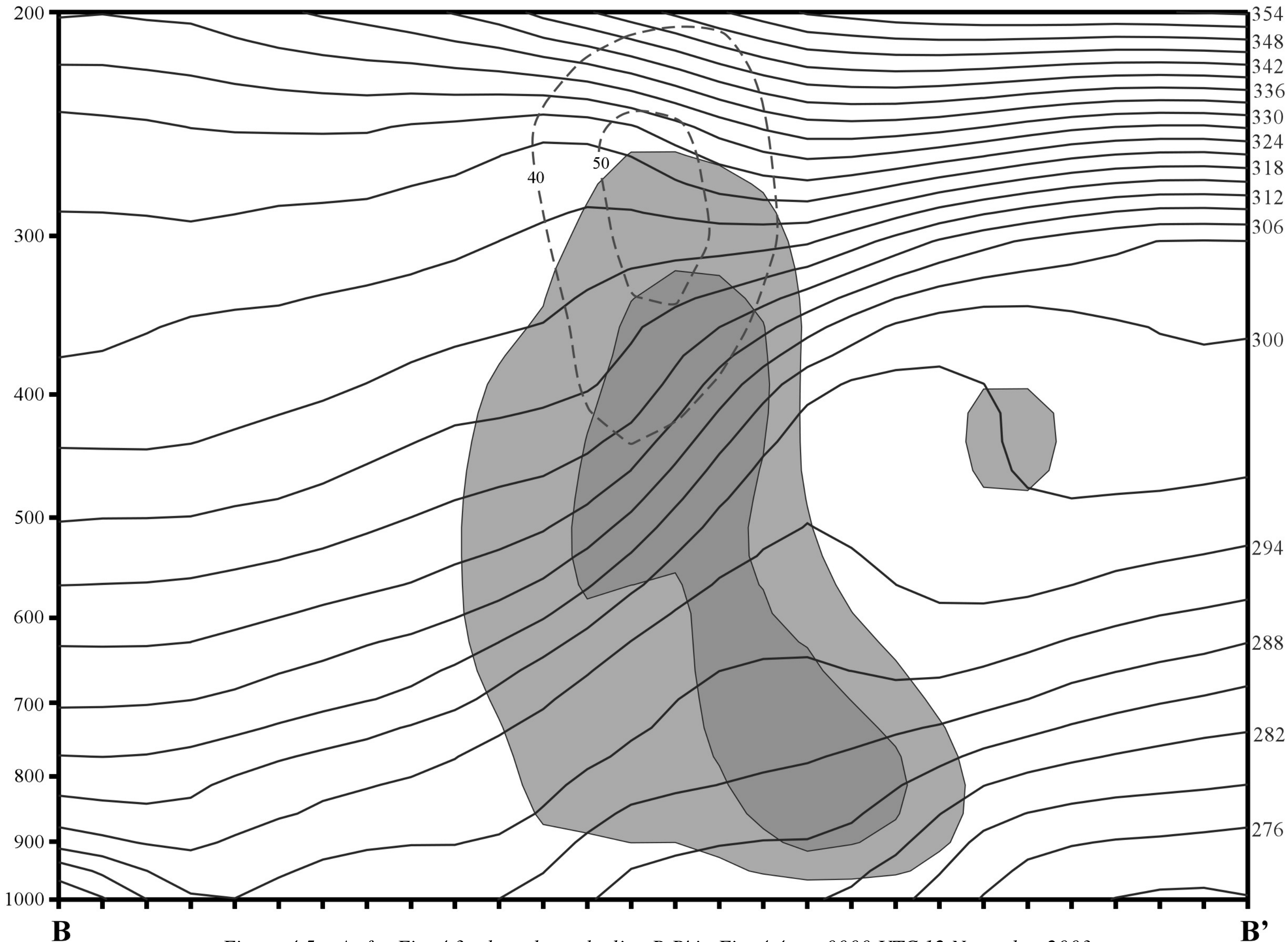

Figure 4.5a: As for Fig. 4.3a, but along the line B-B' in Fig. 4.4a at 0000 UTC 12 November 2003.

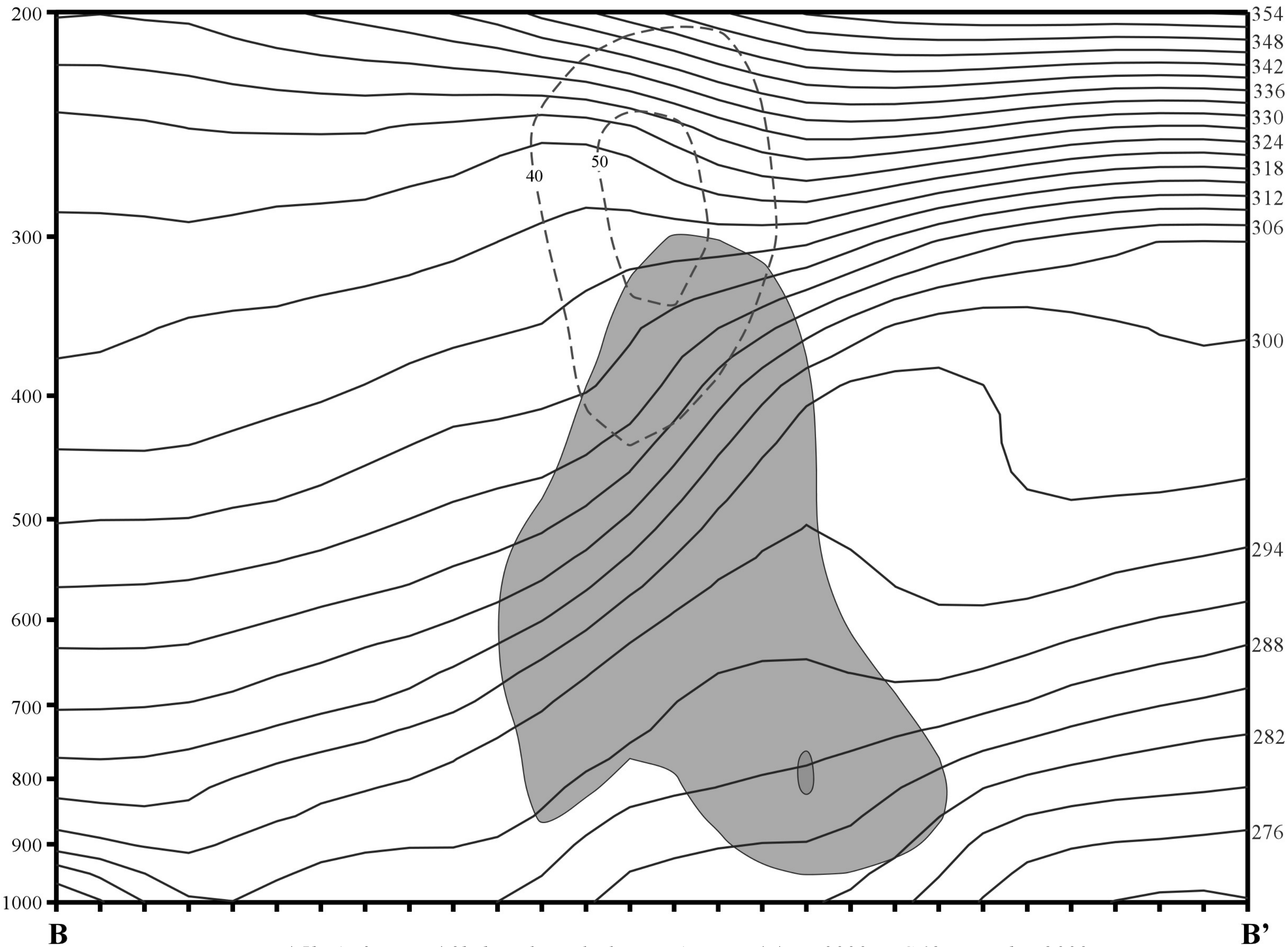

Figure 4.5b: As for Fig. 4.3b, but along the line B-B' in Fig. 4.4a at 0000 UTC 12 November 2003.

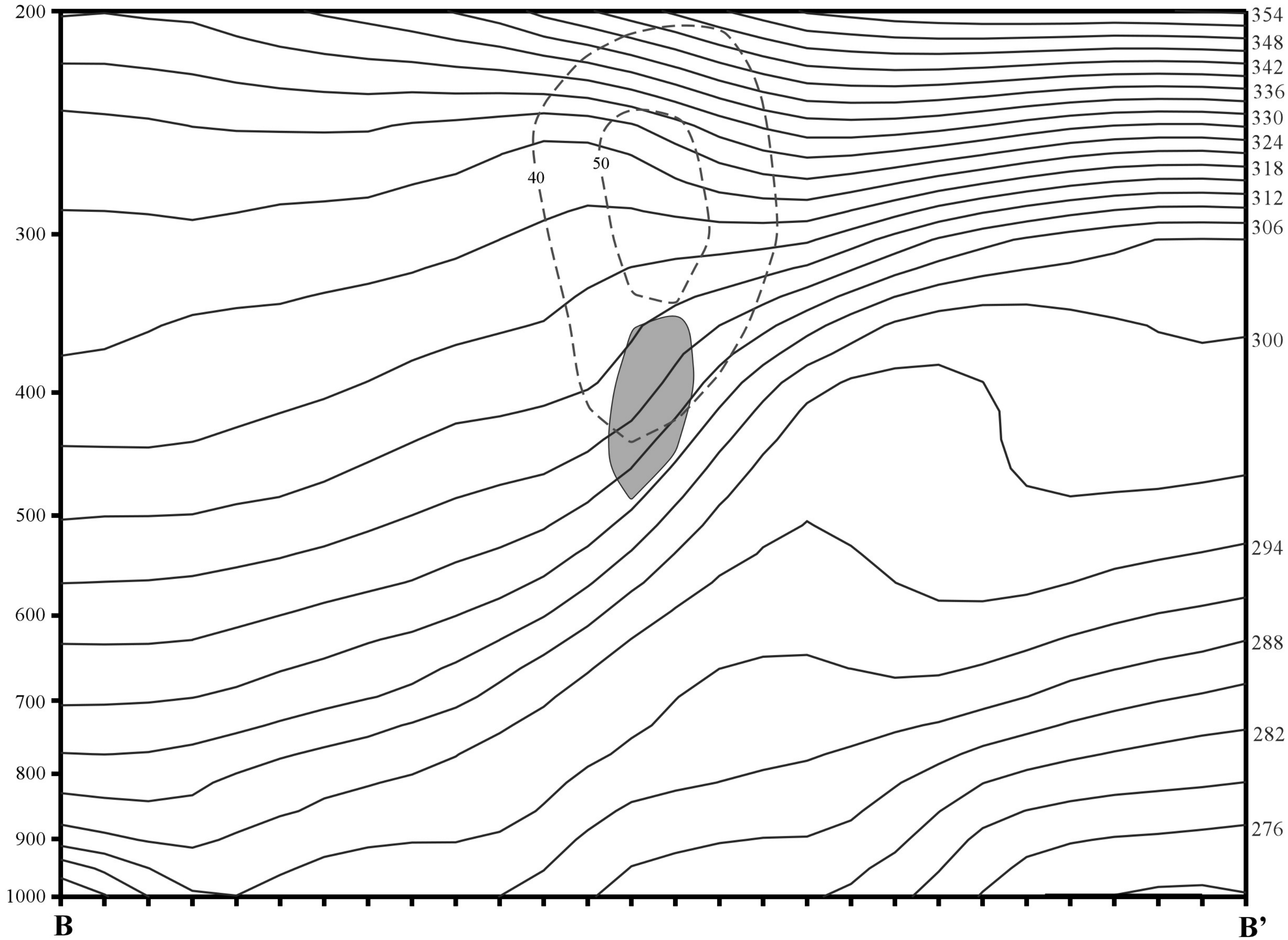

Figure 4.5c: As for Fig. 4.3c, but along the line B-B' in Fig. 4.4a at 0000 UTC 12 November 2003.

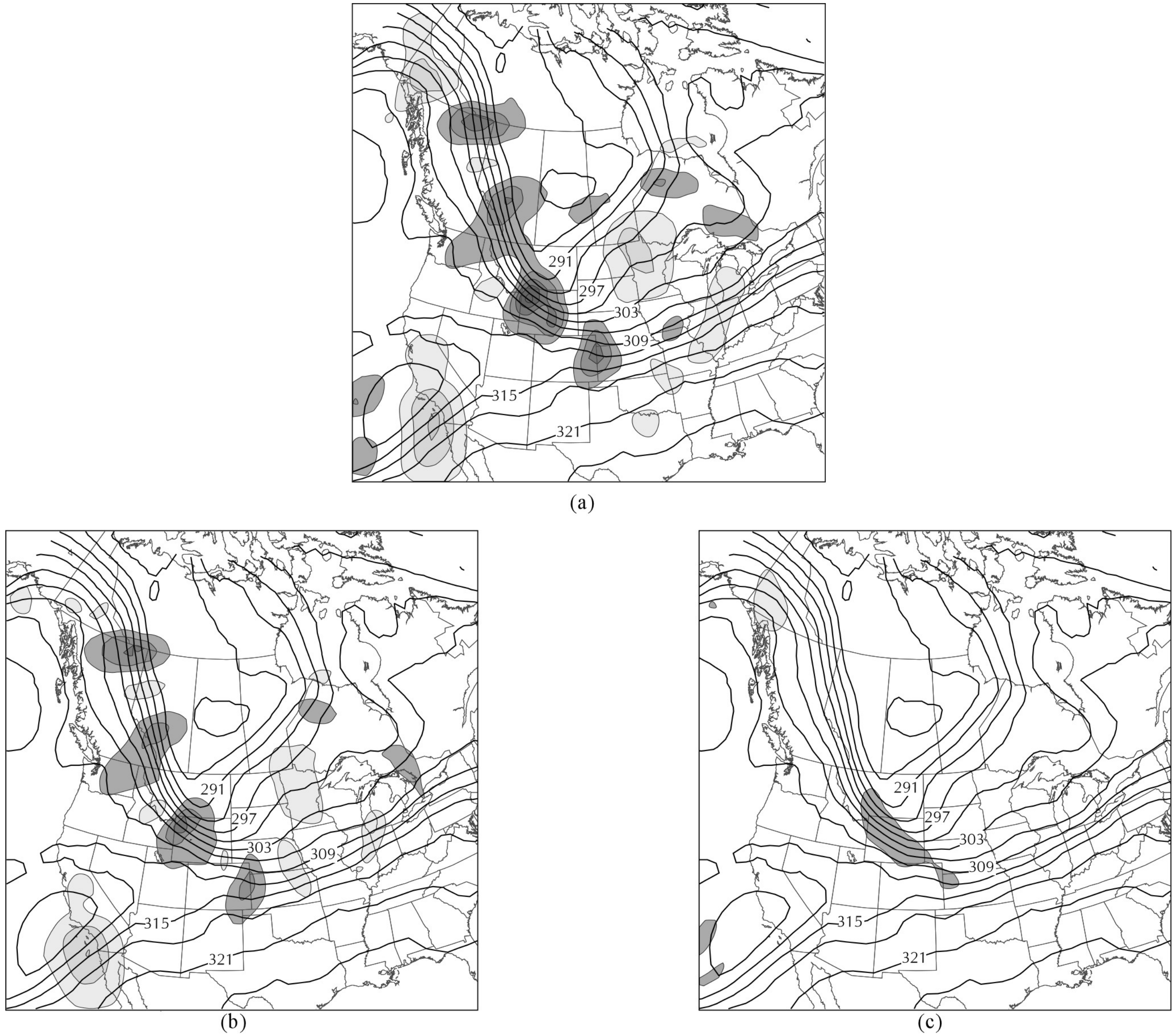

Figure 4.6: As Fig. 4.1, but for 0600 UTC 12 November 2003.

4.6c).

The distribution of vertical motion was very similar at 1200 UTC 12 November, with an amplified region of subsidence in the frontal zone in north central Wyoming (Fig. 4.7a) This pocket of subsidence, with a magnitude of approximately 12 dPa s^{-1}, and a region of weak ascent downstream of the upper-front, formed a couplet that straddled the base of thermal trough in the northern Plains. Shearwise omega was largely responsible for the couplet and continued to contribute the majority of vertical motion associated with the developing upper-front (Fig. 4.7b). However, the contribution by the transverse omega continued to increase, with a band of subsidence oriented along and to the warm side of the most intense portion of the upper-front from central Montana to central Nebraska (Fig. 4.7c).

By 1800 UTC 12 November there was a noticeable change in the QG omega field (Fig. 4.8a). The strongest subsidence had moved into the base of the thermal trough along the South Dakota/Nebraska border and intensified significantly, to approximately 18 dPa s^{-1}. Downstream of the most intense portion of the upper-front, over Minnesota and Wisconsin, the pocket of ascent also intensified to approximately 8 dPa s^{-1}. Shearwise omega continued to account for nearly all of the vertical motion upstream of the thermal trough within the northwesterly flow (Fig. 4.8b). Within the upper-front, which had reached the base of the thermal trough, shearwise omega over Nebraska and South Dakota, contributed approximately 12 dPa s^{-1} of subsidence. Meanwhile, the four quadrants of the southwesterly jet were apparent in the transverse omega field, with the subsidence in the left entrance region contributing roughly 6 dPa s^{-1} to the subsidence within and on the warm side of the southeastern extremity of the upper-front (Fig. 4.8c).

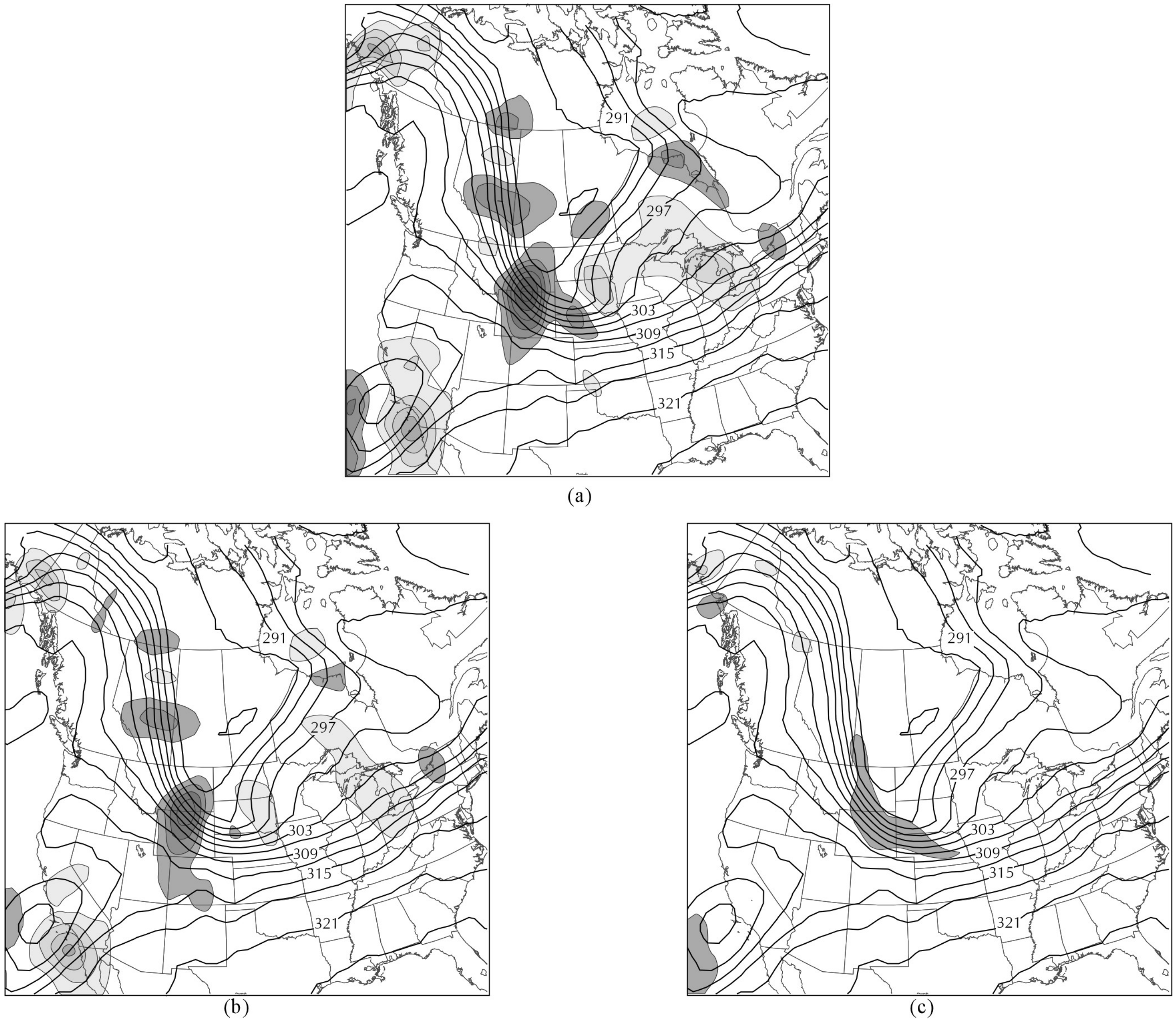

Figure 4.7: As Fig. 4.1, but for 1200 UTC 12 November 2003.

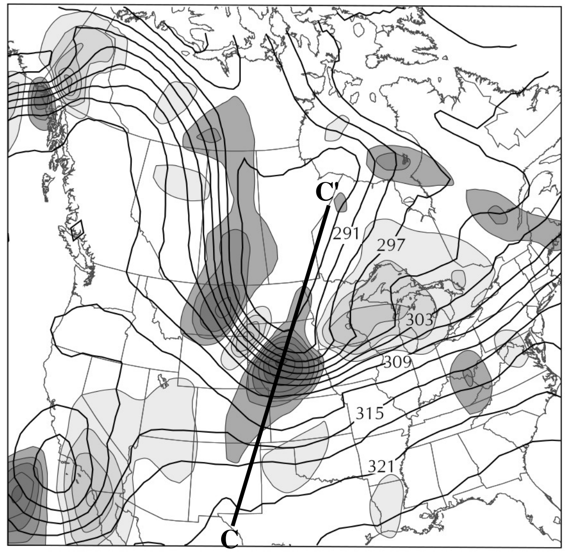

(a)

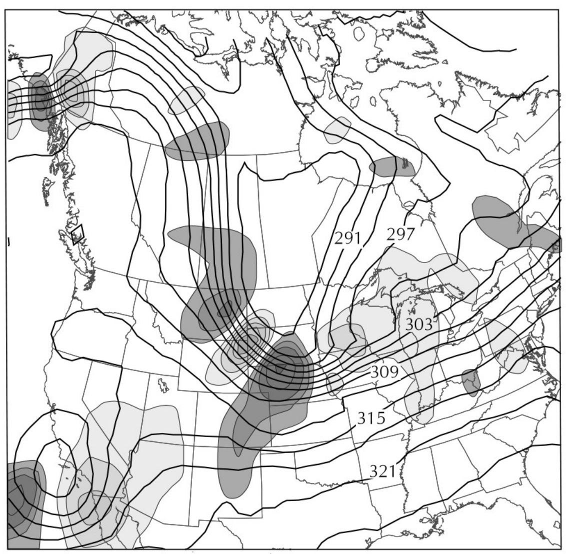

(b)

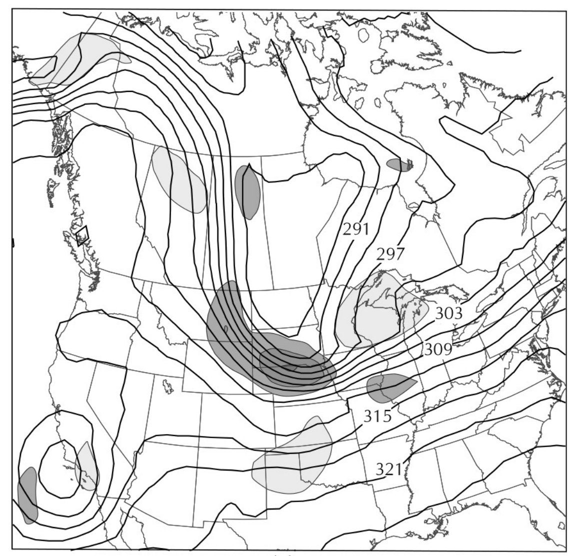

(c)

Figure 4.8: As Fig. 4.1, but for 1800 UTC 12 November 2003 and descent shaded by magnitudes of 2, 4, 6, 9, 12, 15, and 18 dPa s^{-1}.

Several cross sections through the maximum subsidence in northern Nebraska at 1800 UTC 12 November, were taken along the line C-C' in Fig. 4.8a. The total QG subsidence maximum was approximately 12 dPa s^{-1} at 525 hPa, and stretched through the entire depth of the troposphere (Fig. 4.9a). The intense upper-front brought the 303 K isentrope from roughly 350 hPa in Canada to 925 hPa in western Texas. Shearwise omega contributed roughly half of the magnitude of subsidence, with a 6 dPa s^{-1} maximum centered at 500 hPa within the upper-front (Fig. 4.9b). By this time, the thermally direct circulation in the entrance region of the jet streak (Fig. 3.6c) was apparent in the transverse omega field. The center of this circulation was shifted toward the warm side of the upper-front as is the case in regions of cold air advection along the jet axis (Keyser and Pecnick, 1985). The increasing importance of transverse omega to upper frontogenesis is manifested in the significant subsidence (roughly 6 dPa s^{-1}) centered at 600 hPa (Fig. 4.9c). The transverse subsidence in the upper troposphere was positioned in such a way that it aided the upper frontogenesis over the Plains. However, in the lower troposphere, below 550 hPa, the subsidence was on the cold side of the frontal zone, suggesting that the vertical circulation in the lower troposphere was likely contributing to a weakening of the baroclinic zone in that region.

By 0000 UTC 13 November the magnitude of QG ascent downstream of the upper-front surpassed the magnitude of QG subsidence within the upper-frontal zone (Fig 4.10a) which had weakened substantially in the six hour period, to approximately 9 dPa s^{-1}. Strong ascent, roughly 18 dPa s^{-1}, was associated with rapid surface cyclongenesis over the eastern Great Lakes, as described by Martin (2006). This pocket of ascent was primarily associated with shearwise omega (Fig. 4.10b) with some contribution from the transverse

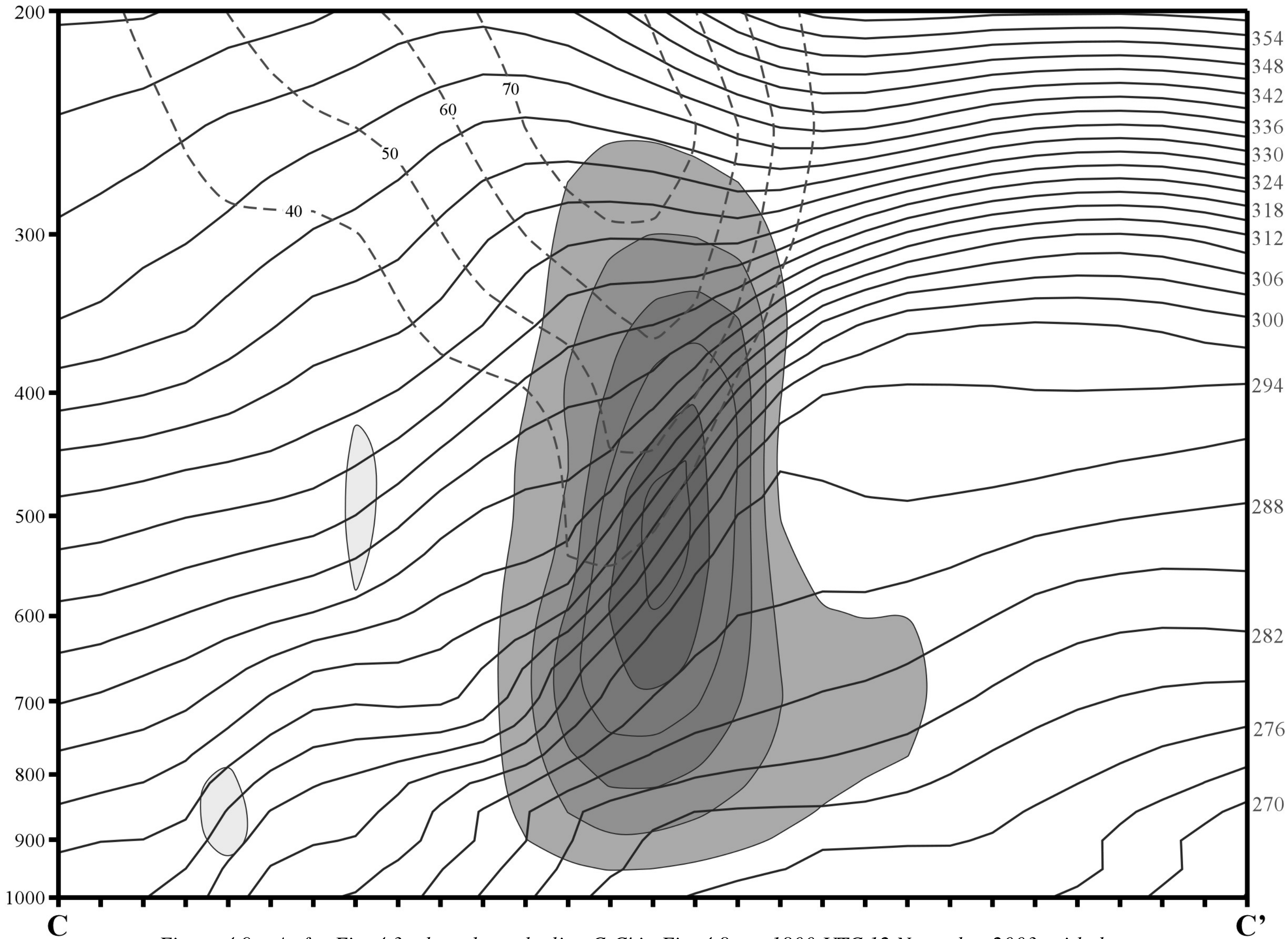

Figure 4.9a: As for Fig. 4.3a, but along the line C-C' in Fig. 4.8a at 1800 UTC 12 November 2003, with descent (ascent) represented by dark (light) shading.

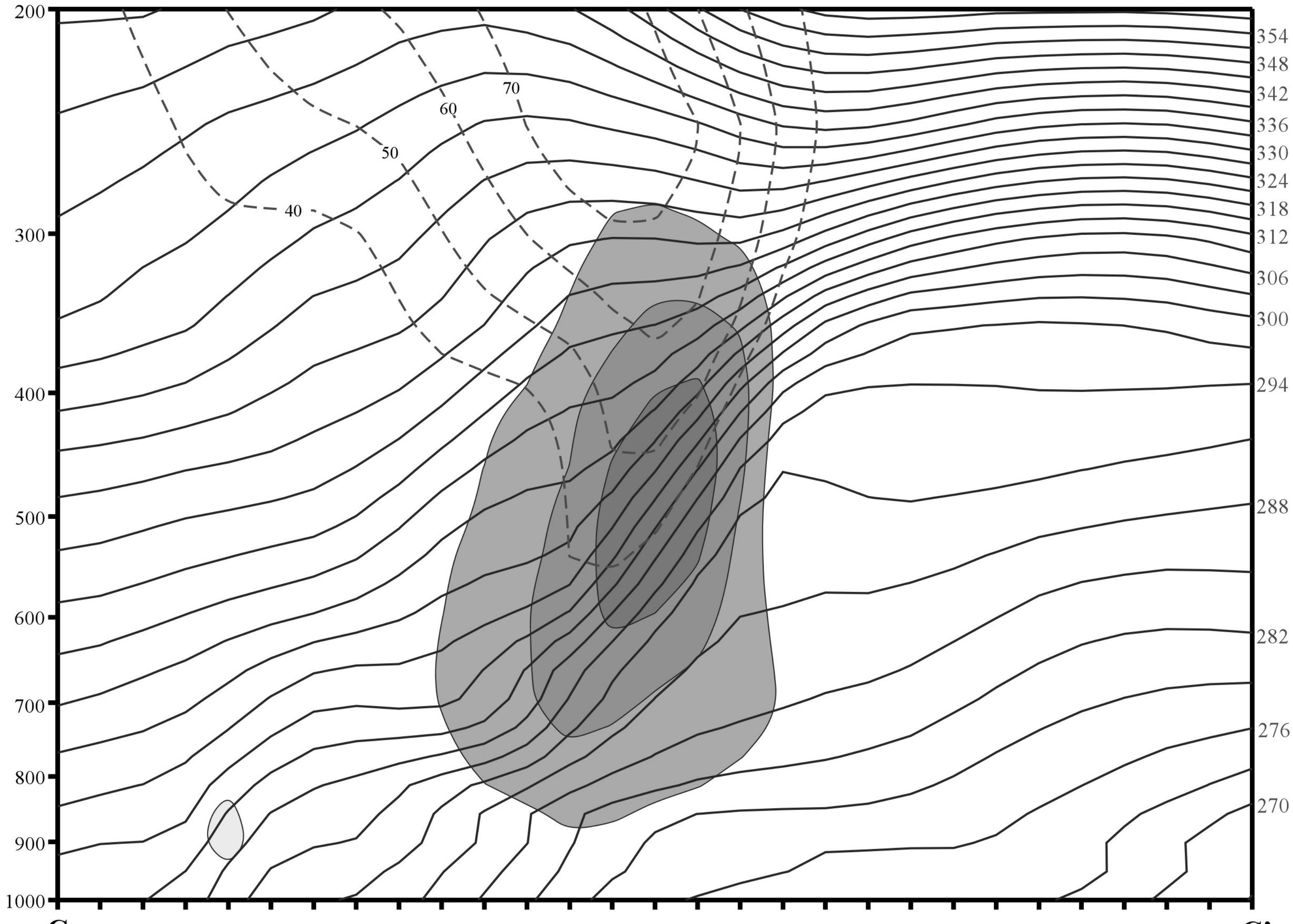

Figure 4.9b: As for Fig. 4.3b, but along the line C-C' in Fig. 4.8a at 1800 UTC 12 November 2003, with descent (ascent) represented by dark (light) shading.

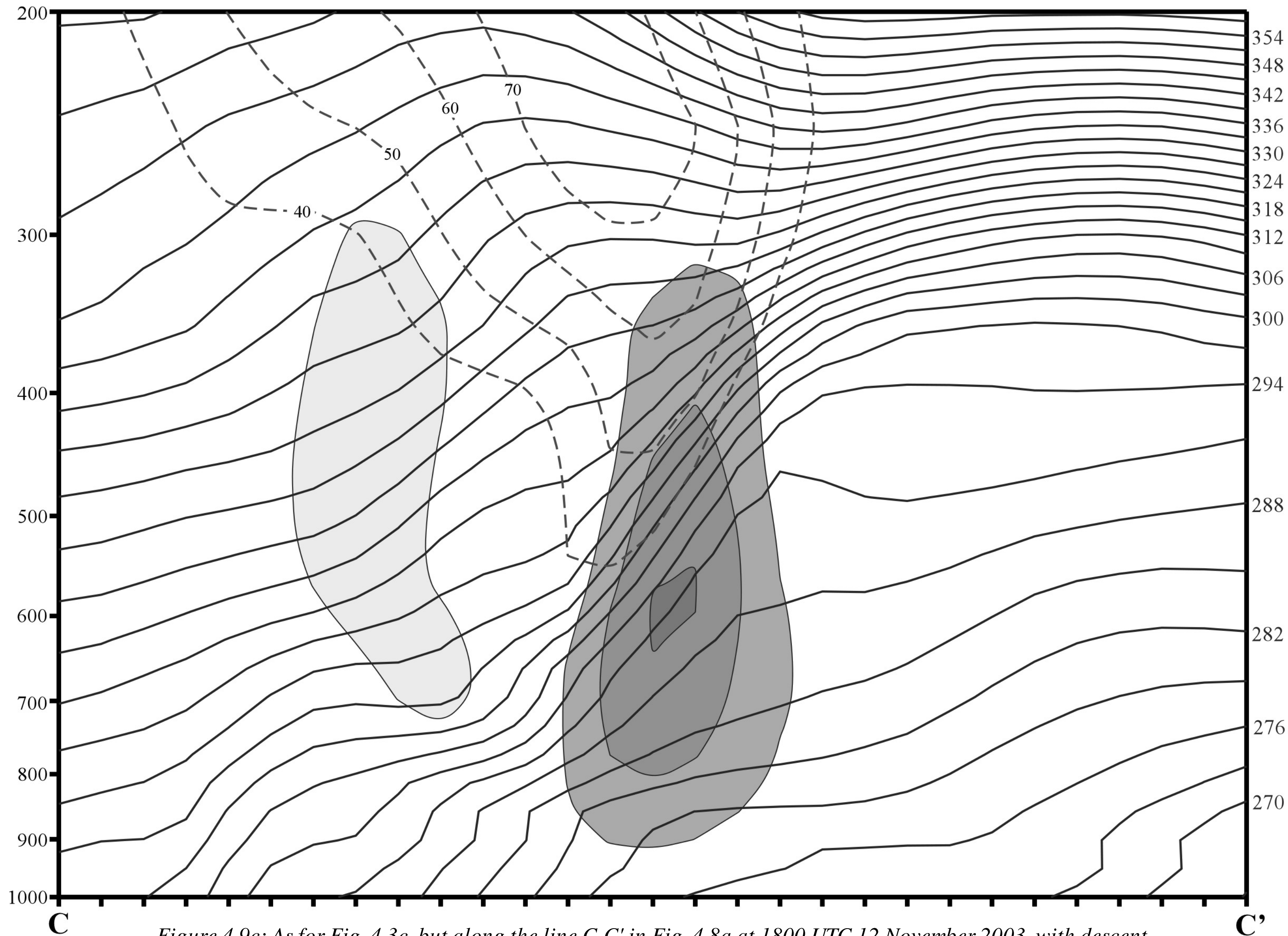

Figure 4.9c: As for Fig. 4.3c, but along the line C-C' in Fig. 4.8a at 1800 UTC 12 November 2003, with descent (ascent) represented by dark (light) shading.

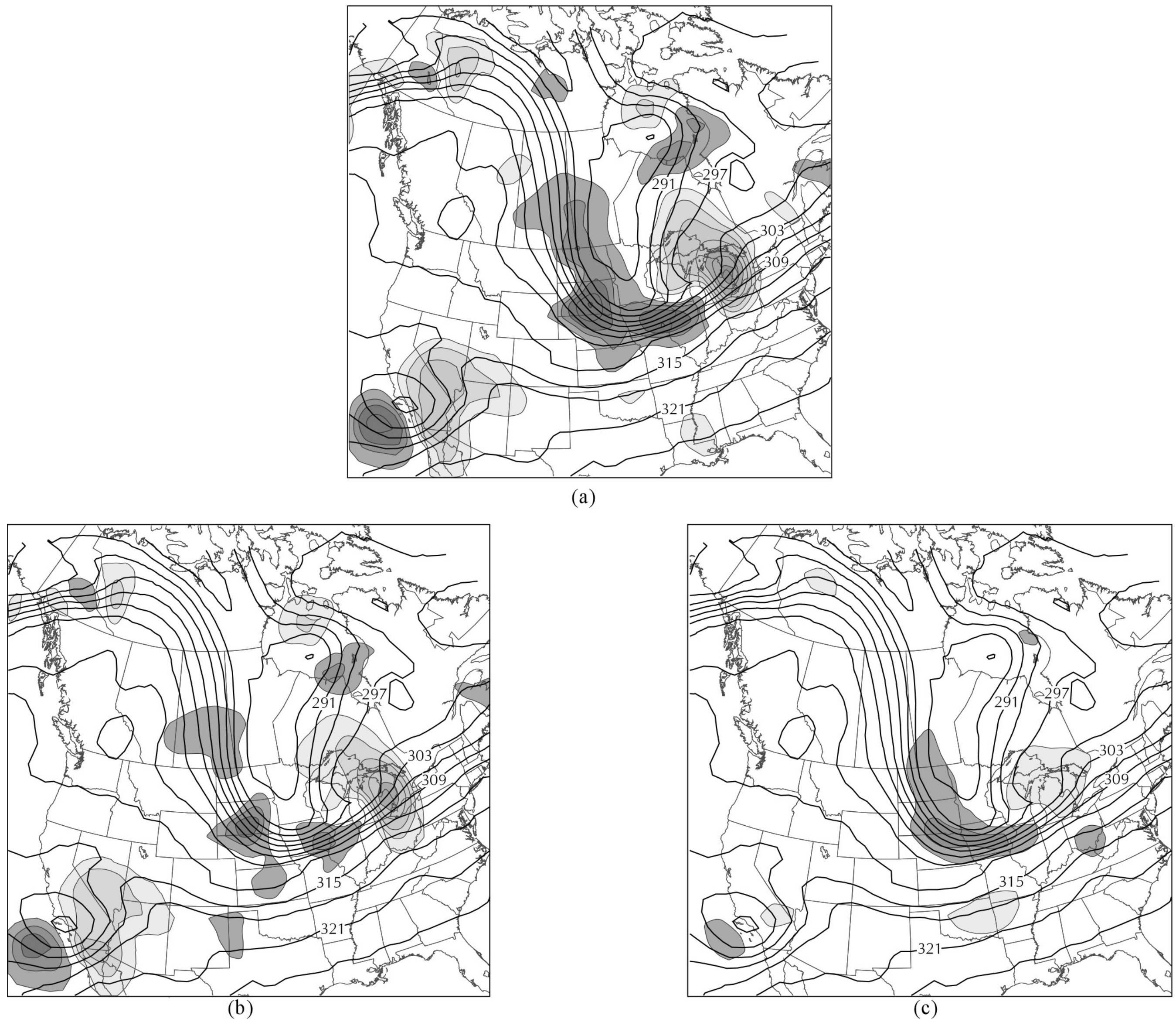

Figure 4.10: As Fig. 4.1, but for 0000 UTC 13 November 2003 and both ascent and descent shaded by magnitudes of 2, 4, 6, 9, 12, 15, and 18 dPa s^{-1}.

ascent (Fig. 4.10c), located in the left exit region of the jet streak. The subsidence was composed of significant contributions from both components of QG omega. Shearwise subsidence described the location of the maxima in southeastern Iowa and South Dakota (Fig. 4.10b), however, the broad band of subsidence over the Midwest, was apparently contained in the transverse subsidence (Fig. 4.10c).

5. Analysis

Partitioning QG vertical motion into shearwise and transverse components provides a more complete picture of the life-cycle of an upper-level front by delineating the connection between the scalar and rotational frontogenesis and their associated vertical circulations. In their work, Schultz and Doswell (1999) explicitly showed the significance of along-front flow variations in the process of upper frontogenesis by describing the importance of rotational frontogenesis in the initiation of the cold air advection and subsequent scalar frontogenesis. The present analysis provides the important frontogenetic vertical motions associated with rotational and scalar frontogenesis, both before and after the initiation of cold air advection along the front. In fact, the present analysis suggests that, with regard to partitioned vertical motion fields during the evolution of this particularly intense upper-front, there are two stages that correspond to the process involved in the initiation of the Shapiro Effect. Stage one can be characterized by a particular pattern of shearwise and transverse motion prior to the onset of cold air advection along the front. While stage two occurs after the onset of cold air advection along the front and is characterized by a notably different vertical motion field.

a. Stage One: Pre-Cold Air Advection

From the QG vertical motion diagnostics presented here, it is evident that for the earliest stage of this case, on 11 November, the vertical motion distribution was dominated by shearwise QG subsidence. Horizontal and vertical sections (Figs. 4.1 – 4.3) revealed that the shearwise subsidence maxima were positioned toward the warm side of the upper-front. This provided the necessary cross-front differential subsidence that produced a region of frontogenetic tilting and the initial development of an upper-front in northwesterly flow. At 0000 UTC and 1200 UTC 11 November, the region of shearwise subsidence at the southernmost extent of the upper-front was the upstream half of a couplet of vertical motion directly associated with a region of positive QG rotational frontogenesis. As suggested by Schultz and Doswell (1999), this positive rotational frontogenesis resulted in a counterclockwise rotation of the isentropes in this region and promoted the development of a thermal trough over western North America. The shearwise QG vertical motion couplet, which represented the secondary circulation associated with the rotation, provided the differential subsidence that allowed for the initial development of the upper-front in the northwesterly flow side of the thermal trough. The continued rotational frontogenesis during this period promoted further intensification of the thermal trough so that it exhibited high amplitude, strongly asymmetric characteristics by 0000 UTC 12 November (Fig. 4.4). This configuration, consistent with the northwesterly flow upper-front conceptual model presented by Schultz and Doswell (1999), allowed for the development of increasing geostrophic cold advection along the upper-front.

Figure 5.1 illustrates the evolution of the 500 hPa geostrophic temperature advection during four periods of the development of this particular upper-front. During the early stage of development, the geostrophic temperature advection was similar to that captured at 1200 UTC 11 November (Fig. 5.1a) and was characterized by sporadic, weak *warm* advection along the length of the upper-front. As the shearwise omega couplet associated with rotational frontogenesis intensified, a region of geostrophic cold air advection developed

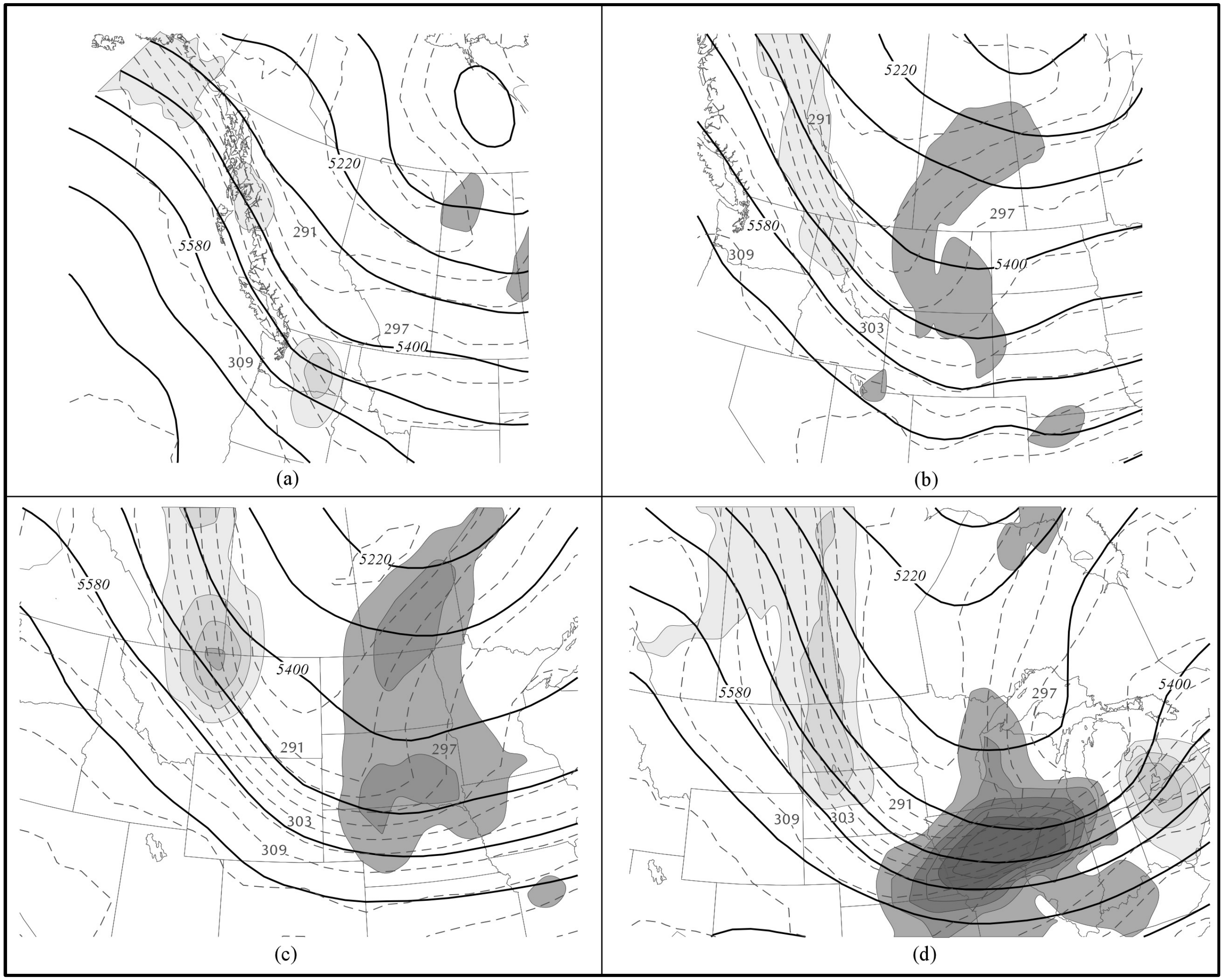

Figure 5.1: The evolution of the 500 hPa geostrophic temperature advection during the development of the 11-13 November 2003 upper-front over North America. Geopotential height in meters (solid lines), isentropes in K (dashed lines), as well as cold (warm) air advection represented by the dark (light) shading, for (a) 1200 UTC 11 November, (b) 0000 UTC 12 November, (c) 1200 UTC 12 November, and (d) 0000 UTC 13 November.

within the thermal trough. By 0000 UTC 12 November weak cold air advection was observed in the vicinity of the high amplitude, strongly asymmetric thermal trough (Fig 5.1b). This configuration signified that the frontogenesis process had moved to stage two.

b. Stage Two: Cold Air Advection

Rotunno et al. (1994) suggested that the onset of cold advection during upper frontogenesis would intensify cross-front $\vec{Q}$ divergence along the shear, which would therefore intensify vertical motions and result in scalar frontogenetic tilting, the *Shapiro Effect*. This process was observed in the later stage of the development of this upper-front, particularly on 12 November. The upper-front, on 12 November, was influenced by a combination of both shearwise and transverse QG omega couplets and characterized by rapid frontogenesis. The ascent and descent of the shearwise omega couplet continued to intensify during this period, allowing the subsidence portion of the couplet to provide an important source of frontogenetic tilting. The associated positive QG rotational frontogenesis also intensified further resulting in stronger cold air advection along the front.

At 1200 UTC 12 November, the temperature advection along the front varied from warm advection in Montana and gradually became a maximum in cold advection in the South Dakota-Nebraska region (Fig. 5.1c). The rotation of the isentropes continued during the latter half of 12 November as couplets of shearwise omega intensified (Figs. 4.7 – 4.10). By 0000 UTC 13 November, the thermal trough and upper-front were robust features of the flow over North America. The strongest cold air advection was positioned over Iowa at the base of the thermal trough within the upper-front itself (Fig 5.1d). The cold advection during this period was positioned in a region of cyclonic shear, which implied frontolytic horizontal geostrophic shear and a forced thermally indirect circulation. This thermally indirect circulation was superimposed on the direct circulation associated with the entrance region of the southwesterly jet and resulted in strong transverse subsidence on the warm side of the upper-front. This transverse circulation thus provided a second source of frontogenetic tilting.

c. Additions to the Schultz and Doswell (1999) Conceptual Model

Figures 5.2 and 5.3 illustrate the characteristic partitioned QG vertical motion fields during the pre-cold air advection and the cold air advection stages of northwesterly flow upper frontogenesis. These figures represent an extension to the Schultz and Doswell (1999) conceptual model (Fig. 2.4) and capture the important coupling of both components of vertical motion in upper frontogenesis.

Figure 5.2a depicts the characteristic QG shearwise vertical motion observed during the pre-cold air advection stage of upper frontogenesis in northwesterly flow. Regions of frontogenetic shearwise subsidence are scattered along the length of a developing upper-front, with the southernmost region of subsidence coupled with a region of shearwise ascent. This couplet is associated with the region of positive rotational frontogenesis that rotates the isentropes cyclonically in that region and thus initiates the cold air advection along the front. Figure 5.2b represents the cold air advection stage of upper frontogenesis and implies strong cold air advection at the base of the trough. As the upper-front intensifies from the pre-cold advection stage to the cold advection stage, the vorticity maximum associated with the upper-

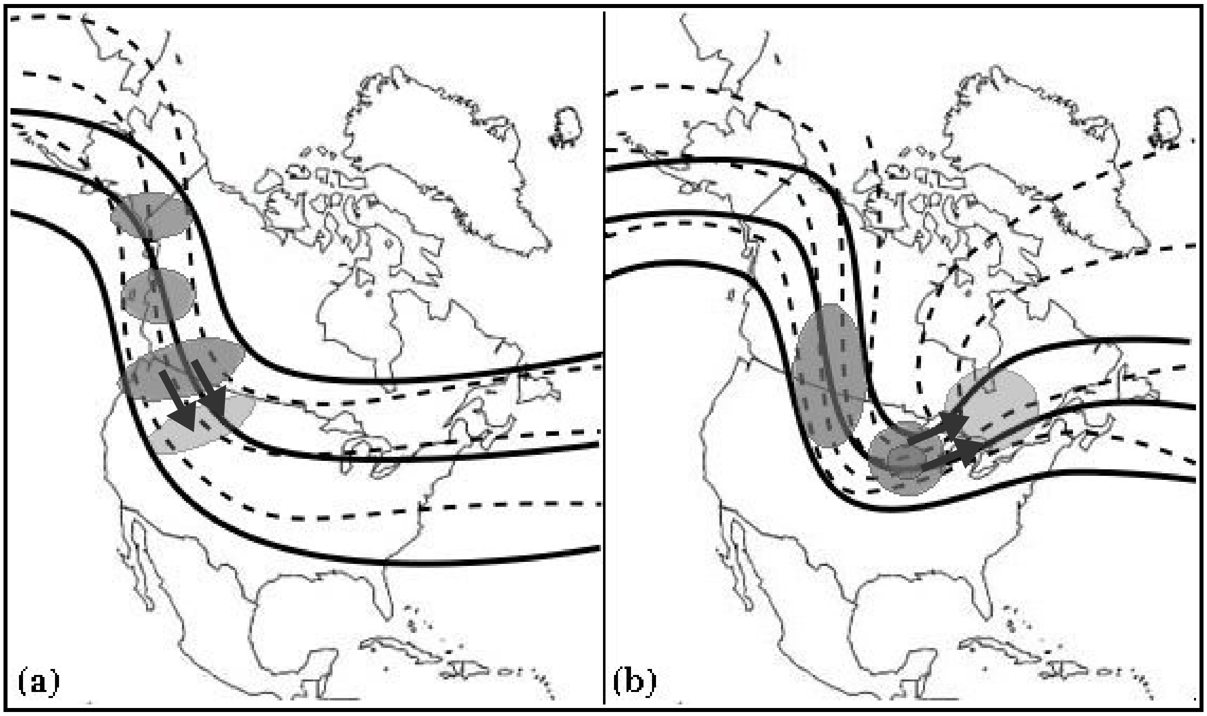

Figure 5.2: The characteristic shearwise QG vertical motion (ω_s) fields during the (a) pre-cold air advection and the (b) cold air advection stages of northwesterly flow upper frontogenesis. Dashed lines represent isentropes and solid lines represent the geopotential height at approximately the 500 hPa surface. Dark (light) shading represents characteristic subsidence (ascent) during these stages of upper frontogenesis, while the arrows represent characteristic rotational frontogenesis ($\boldsymbol{Q}_s$) vectors..

front also intensifies, as depicted in the Schultz and Doswell conceptual model (Fig. 2.4). Martin (1999 and 2006) noted that a large part of ω_s is captured by forcing from vorticity advection by the thermal wind. Consequently, the intensifying frontal zone and the intensifying vorticity maximum led to stronger positive and negative vorticity advection by the thermal wind and stronger positive rotational frontogenesis (as described by Schultz and Doswell), thus supporting the observed intensification of the ω_s couplet from the pre-cold advection stage to the cold advection stage of frontogenesis. Fig. 5.2b also depicts the intensifying shearwise vertical motion, characterized by stronger subsidence within the intense upper-front itself as well as stronger ascent downstream of the thermal trough. It is

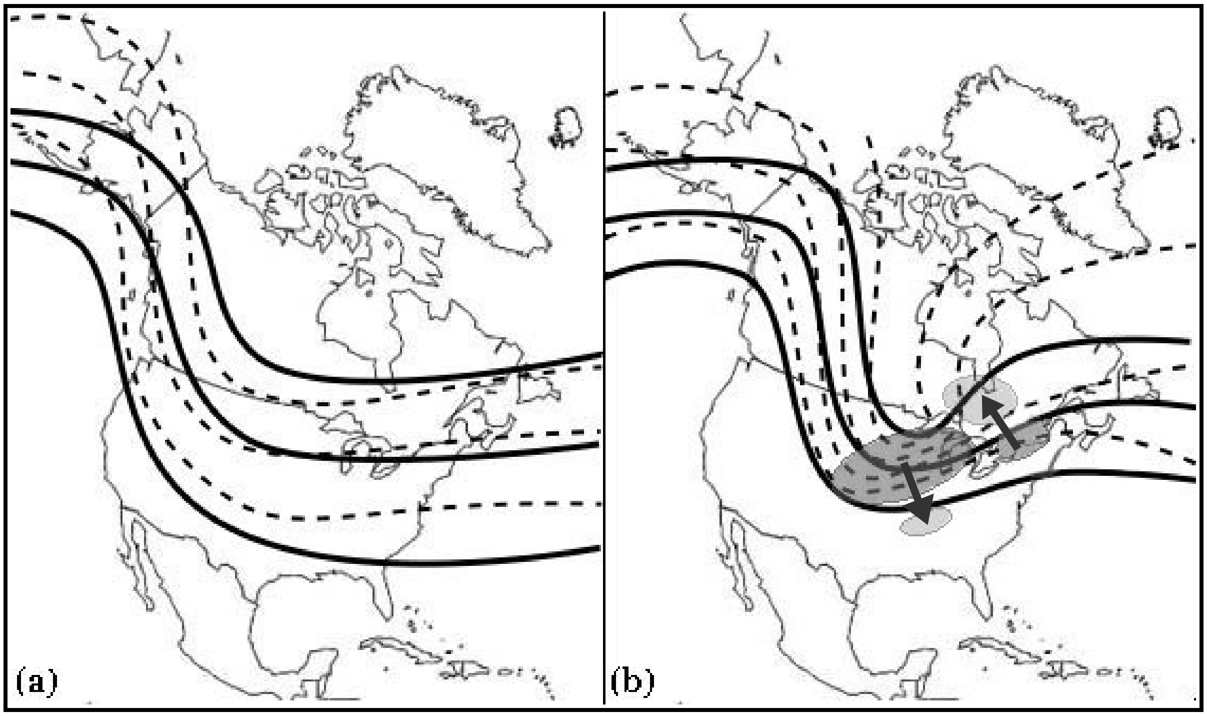

Figure 5.3: As Fig. 5.2, but for transverse QG vertical motion (ω_n) fields and the scalar frontogenesis ($\boldsymbol{Q}_n$) vectors.

clear that shearwise subsidence plays a major role in both stages of upper frontogenesis.

Figure 5.3a represents the QG transverse vertical motion during the pre-cold air advection stage of upper frontogenesis in northwesterly flow. Transverse motion, associated with scalar frontogenesis, plays no role during this period. However, with the onset of cold air advection, transverse circulations develop (Fig. 5.3b). In the base of the thermal trough, a local thermally indirect circulation is forced in the region of cold air advection along the front. However, this circulation is superimposed upon a thermally direct circulation in the entrance region of an intensifying jet and results in a region of subsidence maximized beneath the jet core, to the warm side of the upper-front itself. A portion of this region of transverse subsidence coincides with a region of shearwise subsidence (just upstream of the thermal trough axis), and their circulations combine to produce intense frontogenetic tilting and a period of rapid frontogenesis.

These figures illustrate the importance of shearwise vertical motions,ω_s, in upper frontogenesis. Even during a period of peak frontogenesis, the type of vertical motion traditionally assumed to drive upper frontogenesis, ω_n, only accounts for roughly half of the frontogenetic subsidence. Variations, such as curvature, along the flow can not be neglected at any time during the development of an upper-front. During the early stages of the life-cycle depicted here, the QG rotational frontogenesis initiated the development of cold advection along the front while the associated shearwise subsidence initiated the development of the upper-front itself. Found in a region of horizontal geostrophic shear, the developing cold air advection consequently forced a secondary transverse vertical circulation, which provided additional frontogenetic tilting. Thus, the rapid frontogenesis resulted from the fact that the necessary rotational frontogenesis is itself associated with a vertical circulation that produces secondary frontogenetic tilting.

6. Conclusion

a. Summary

Palmen and Nagler (1949) were the first to allude to the idea that the total vertical motion might be usefully separated into two categories based upon the distribution of along- and across-front forcing. They suggested that a combination of these two types of vertical motions would have an important influence on the evolution of upper-level frontal zones. Early research on the process of upper frontogenesis by Reed and Sanders (1953) suggested that the basic mechanism in the creation of an upper-level front was isentropic tilting due to cross-front differential subsidence. Sawyer (1956) and Eliassen (1962) provided a two-dimensional circulation equation that captured what was thought to be at the heart of the upper frontogenesis problem, the cross-front, transverse ageostrophic vertical circulation. Three-dimensional numerical simulations of upper-fronts from the real atmosphere, by Newton and Travisan (1984a,b), suggested that the inclusion of modifications to the transverse ageostrophic vertical circulation induced by flow curvature was significant and could not be neglected during the life-cycle of an upper-front. They noted that a combination of transverse and curvature-induced vertical circulations more completely accounted for frontogenesis than did either type of circulation alone. Work by Keyser et al. (1992a) provided a generalization of the QG form of the Sawyer-Eliassen equation, applicable to three-dimensions, in which they separated the three-dimensional vertical circulation into two two-dimensional vertical circulations in orthogonal vertical planes, that were oriented in the along- and cross-front directions. Following their work, Keyser et al. (1992b) provided a method of diagnosing the two types of vertical motions, corresponding to the along- and cross-front directions, using the **Q**-vector form of the QG omega equation. These two components of the QG omega are referred to as transverse and shearwise omega in this thesis and are associated with the across- and along-isentrope components of the QG vector frontogenesis function, **Q**, respectively. Transverse omega, ω_n, is associated with processes that will intensify or weaken $|\nabla\theta|$ (i.e., QG scalar frontogenesis), while shearwise omega, ω_s, is associated with processes that will rotate $\nabla\theta$ (i.e., QG rotational frontogenesis).

The first conceptual model of the evolution of an upper-front through a baroclinic wave by Shapiro (1982), suggested that cold air advection in northwesterly (cyclonic) flow was a favorable circumstance for the production of frontogenetic vertical tilting. This suggestion was later proven in the idealized experiment of Keyser and Pecnick (1985). Following Shapiro (1982), Schultz and Doswell (1999) suggested that in northwesterly flow, rotational frontogenesis was responsible for a cyclonic rotation of the isentropes that initiated cold air advection along the length of a developing upper-front. The resulting cold air advection, when present in an environment of cyclonic shear, forced a thermally-indirect circulation that promoted positive scalar frontogenesis. Schultz and Doswell (1999) were not, however, able to isolate the secondary vertical circulations associated with the important rotational frontogenesis. The current analysis extends their work by examining, from a QG perspective, the important ω_s and ω_n associated with the rotational and scalar frontogenesis, respectively, during upper frontogenesis. We document the evolution of an upper-front in northwesterly flow and the initiation of cold air advection along the front. By categorizing the evolution of this upper-front into *pre-cold air advection* and *cold air advection* stages, we describe particularly robust patterns of both ω_s and ω_n observed during the life-cycle of an upper-level front.

During the first stage, the *pre-cold air advection* stage, rotational frontogenesis was responsible for initiating the cold air advection the upper-front and was also responsible for forcing ω_s subsidence in a region favorable to upper frontogenesis. This subsidence was responsible for the initial development of the upper-front itself. The ω_s was the only type of vertical motion observed during the first stage of development. The second stage of development, the *cold air advection* stage, began once cold air advection along the front was established. During this stage, ω_n couplets, with subsidence maximized beneath the jet core, developed in the regions of cold air advection along the front, a process previously described as the Shapiro Effect. These couplets were superimposed on the already robust ω_s couplets, resulting in a period of enhanced frontogenetic tilting. Thus, rapid frontogenesis during the evolution of this upper-front resulted from the fact that rotational frontogenesis was itself associated with a vertical circulation that produced a secondary frontogenetic tilting.

b. Future Work

This work has opened the door to some interesting research questions. For example, the body of work by Uccellini et al. (1985), Sanders (1988) and Lackmann et al. (1997) makes the case that upper-level precursor disturbances to surface cyclogenesis are very often direct consequences of the upper frontogenesis process itself. Would it be possible to determine what type (rotational or scalar) of upper frontogenesis is responsible for the creation of these upper-level precursor disturbances? Lackmann et al. (1997) noted that the production of vorticity in a mid-tropospheric jet-front system and the subsequent compaction of the vorticity feature suggests a link between mid-tropospheric frontogenesis and the creation of an upper-trough, a common type of precursor to surface cyclogenesis. Using a scale analysis of the vorticity equation, they found that the vertical advection, stretching, and tilting terms accounted for the majority of the vorticity production within an upper-level jet-front system. These important terms are all dependent on vertical motion. This led Lackmann et al. (1997) to emphasize the importance of the transverse vertical circulations, associated with scalar frontogenesis, in steepening and lowering the dynamic tropopause while producing vorticity in the upper-level precursor prior to surface cyclogenesis. However, our current work reveals the importance of shearwise omega during rapid upper-level frontogenesis. By documenting the vorticity production associated with forcing from ω_s and ω_n, separately, future work could illustrate the influence of both rotational and scalar frontogenesis on the genesis of an upper-level precursor disturbances.

Another question stems from the fact that subsidence is at the heart of upper frontogenesis and can be strong enough to bring air with stratospheric characteristics deep into the troposphere in a stratospheric intrusion. What is going on in the lower stratosphere, above these upper-level fronts, in the source region of the subsiding air? The nature of the lower stratospheric portion of these upper-level jet-front systems has been debated in the literature since the 1950s. The upper tropospheric portion of these systems is rather well agreed upon now—this is not true for the lower stratospheric portion. The last argument of this "structure" debate was provided by Shapiro (1981), in which he discussed observational research aircraft data suggesting a hyper-gradient in temperature within the lower stratospheric meso-scale cyclonic shear zone above the jet core. This region contained all the characteristic signatures of a frontal zone, including (1) enhanced temperature gradient, (2) cyclonic vorticity maximum, and (3) enhanced static stability. However, it was not then, and has never been, referred to as a front. Should it be referred to as a front, perhaps the *lower stratospheric front*? What role do the circulations about such a lower-stratospheric frontal feature play in the evolution of the whole jet-front system? Preliminary work suggests a coupling of the upper tropospheric and lower stratospheric frontal circulations, so that the forcing for the subsidence that creates the stratospheric intrusions may originate in the lower stratosphere, well above the jet core. In addition, we have noted several cases worth investigating, including 10-13 November 2003 and 28 January to 4 February 2007, in which the lower stratospheric development, in terms of an increase in the horizontal temperature gradient on an isobaric surface, seems to precede upper tropospheric development. Whether or not this set of circumstances is characteristic of the comprehensive life-cycle of upper tropospheric jet/front systems in clearly an outstanding question of great scientific and operational relevance. Further investigations of this type will surely provide new insight into the evolution, structure, and life-cycle of these intriguing jet-front systems.

References

Andrews, D. G., J. R. Holton, and C. B. Leovy, *Middle Atmosphere Dynamics*, 489 pp., Academic, San Diego, Calif., 1987.

Beebe, R. G. and F. C. Bates, 1955: A mechanism for assisting in the release of convective instability. *Mon. Wea. Rev.* **83**, 1-10.

Bjerknes, J., 1926: The structure of fronts. *Meteor. Mag.,* **61**, 32–33.

_______ 1951: Extratropical cyclones. Pp. 577-598 in *Compendium of Meteorology*. Ed. T. F. Malone. American Meteorological Society. Boston, MA, USA.

______ and E. Palmen, 1937: Investigation of selected European cyclones by means of serial ascents. *Geofys. Publ.*, **12**(2), 1-12.

______ and H. Solberg, 1922: Life cycle of cyclones and the polar front theory of atmospheric circulation. *Geofys. Publ.,* **1**(3), 1-18.

Bosart, L. F., (1970): Mid-tropospheric frontogenesis: *Quart. J. Roy. Meteor. Soc.,* **96,** 442–471.

Cammas, J. P. and D. Raymond, 1989: Analysis and diagnosis of the composition of ageostrophic circulation in jet-front systems. *Mon. Wea. Rev.* **117**, 2447-2462.

Danielsen, E. F., 1964: Project Springfield Report. DASA 1517. Defence Atomic Support Agency.

Eliassen, A., 1962: On the vertical circulation in frontal zones. *Geofys. Publ.*, **24**(4), 147-160.

Hess, S. L., 1948: Some new mean meridional cross sections through the atmosphere. *J. Meteor.*, **5**(6), 293-300.

Hoskins, B. J. and F. P. Bretherton, 1972: Atmospheric frontogenesis models: Mathematical formulation and solution. *J. Atmos. Sci.*, **29**, 11-37.

______, I. Draghici, and H. C. Davies, 1978: A new look at the ω-equation. *Quart. J. Roy. Meteo. Soc.*, **104**, 31-38.

Keyser, D. and M. J. Pecnick, 1985: A two-dimensional primative equation model of frontogensis forced by confluence and horizontal shear. *J. Atmos. Sci.*, **42**, 1259-1282.

______, M. J. Reeder, and R. J. Reed, 1988: A generalization of Petterssen's frontogenesis function and its relation to the forcing of vertical motion. *Mon. Wea. Rev.* **116**, 762-780.

______, B. D. Schmidt and D. G Duffy, 1992: Quasigeostrophic vertical motions diagnosed from along- and cross-isentrope components of the Q vector. *Mon. Wea. Rev.,* **120**(5), 731–741.

______ and M. A. Shapiro, 1986: A review of the structure and dynamics of upper-level frontal zones. *Mon. Wea. Rev.,* **114**, 452-499.

Lackmann, G. M., D. Keyser, and L. F. Bosart, 1997: A characteristic life cycle of upper-tropospheric cyclogenetic precursors during the Experiment on Rapidly Intensifying Cyclones over the Atlantic (ERICA). *Mon. Wea. Rev.*, **125**, 2729-2758.

Martin, J. E., 1999: Quasigeostrophic forcing for ascent in the occluded sector of cyclones and the Trowal airstream. *Mon. Wea. Rev.* **127**, 70-88.

______, 2006: The role of shearwise and transverse quasigeostrophic vertical motions in the midlatitude cyclone life cycle. *Mon. Wea. Rev.* **134**, 1174–1193.

______, 2007: Lower-tropospheric height tendencies associated with the shearwise and transverse components of quasigeostropic vertical motion. *Mon. Wea. Rev.* **135**, 2803–2809.

Miller, J. E., 1948: On the concept of frontogenesis. *J. Meteor.*, **5**, 169-171.

Namias, J. and P. F. Clapp, 1949: Confluence theory of the high troposphere jet stream. *J. Meteor.*, **6**, 330-336

Newton, C. W., and A.V. Persson, 1962: Structural characteristics of the subtropical jet stream and certain lower-stratospheric wind systems. *Tellus*, **14**, 221-241.

Newton, C. W, and A. Trevisan, 1984a: Clinogenesis and frontogenesis in jet-stream waves. Part I: Analytical relations to wave structure. *J. Atmos. Sci.*, **44**, 2717-2734.

______ and A. Trevisan, 1984b: Clinogenesis and frontogenesis in jet-stream waves. Part II:

Channel mode numerical experiments. *J. Atmos. Sci.*, **44**, 2735-2755.

Palmén, E., 1948, On the distribution of temperature and wind in the upper westerlies. *J. Meteor.*, **5**, 20-27.

______ and K. M. Nagler, 1949: The formation and structure of large-scale disturbances in the westerlies. *J. of Meteor.,* **6**(4), 227-242.

Petterssen, S., 1936: Contribution to the theory of frontogenesis. *Geofys. Publ.*, **11**(6), 1-27.

Reed. R. J., 1955: A study of a characteristic type of upper-level frontogenesis. *J. Meteor.*, **12**, 226-237.

______ and F. Sanders, 1953: An investigation of the development of a mid-tropospheric frontal zone and its associated vorticity field. *J. Meteor.*, **10**, 338-349.

Reeder, M. J. and D. Keyser, 1988: Balanced and unbalanced upper-level frontogenesis. *J. Atmos. Sci.* **45**(22), 3366–3386.

Reiter, E. R., 1969: *Jet Stream Meteorology*. The University of Chicago Press, 515 pp.

Sanders, F., 1988: Life history of mobile troughs in upper westerlies. *Mon. Wea. Rev.* **116**, 2629–2648.

Sawyer, J. S., 1956: The vertical circulation at meteorological fronts and its relation to frontogenesis. *Proc. Roy. Soc. London*, **A234**, 346-362.

Schultz, D. M. and C. A. Doswell, 1999: Conceptual models of upper-level feontogenesis in south-westerly and north-westerly flow. *Quart. J. Roy. Meteor. Soc*, **125**, 2535-2562.

Shapiro, M. A., 1970: On the applicability of the geostrophic approximation to upper-level frontal-scale motions. *J. Atmos. Sci.*, **27**, 408-420.

Shapiro, M. A., 1981: Frontogenesis and geostrophically forced secondary circulations in the vicinity of jet stream-frontal zone systems. *J. Atmos. Sci.*, **38**, 954-973.

______, 1982: Mesoscale weather systemsof the central United States. *The National STORM Program: Scientific and Technological Bases and Major Objectives*, R. A. Anthes, Ed., University Corporation for Atmospheric Research, Boulder, CO. USA

Shapiro, M. A. and P. J. Kennedy, 1981: Research aircraft measurements of jet stream geostrophic and ageostrophic winds. *J. Atmos. Sci.*, **38**, 2642-2652.

Sutcliffe, R. C., 1939: Cyclonic and Anticyclonic development. *Quart. J. Roy. Meteor. Soc.*, **65**, 518-524.

Uccellini, L. W., and D. R. Johnson, 1979: The coupling of upper and lower tropospheric jet streaks and the implications for the development of severe convective storms. *Mon. Wea. Rev.*, **107**, 682-703.

______, D. Keyser, K. F. Brill, and C. H. Wash, 1985: The President's Day cyclone of 18-19 February 1979: Influence of upstream trough amplification and associated tropopause folding on rapid cyclogenesis. *Mon. Wea. Rev.*, **113**, 962-988.